Authigenic carbonates in the upper Miocene sediments of the Tertiary Piedmont Basin (NW Italy): vestiges of an ancient gas hydrate stability zone ?

AUTHIGENIC CARBONATES IN THE UPPER MIOCENE SEDIMENTS OF THE TERTIARY PIEDMONT BASIN (NW ITALY): VESTIGES OF AN ANCIENT GAS HYDRATE STABILITY ZONE ?

Francesco Dela Pierre [1, 2], Luca Martire [1], Marcello Natalicchio [1], Pierangelo Clari [1] and Catalin Petrea [1]

1) Dipartimento di Scienze della Terra, Università di Torino. Via Valperga Caluso, 35 – 10125 Torino, Italy.

2) CNR – Istituto di Geoscienze e Georisorse. Via Valperga Caluso 35 – 10125, Torino - Ita

ABSTRACT

A wide array of carbonate-rich rocks has been recognized in the Tertiary Piedmont Basin (NW Italy), hosted in lower Messinian slope deposits. Carbonate cements show negative $\delta^{13}C$ values and positive $\delta^{18}O$ ones, suggesting that carbonate precipitation was induced by microbial degradation of methane sourced by gas hydrate destabilisation. Two groups of rocks have been distinguished: 1) *Lucina*-bearing mud breccias, representing the sea floor product of an ancient seepage site; 2) *Lucina*-free concretions originated below the sediment-water interface. Within this group, two subtypes have been further distinguished: a) stratiform concretions; b) cylindrical concretions.

Stratiform concretions result from precipitation of dolomite in the pores of muddy sediments. Some of them display a brecciated structure, others show a network of septarian- like cracks that are empty, filled with sediments or zoned carbonate cements. Their internal features are related to the formation of gas hydrates within the sediments and to their destabilisation. Thus, these rocks mark a portion of the sedimentary column located within a (paleo) gas hydrate stability zone (GHSZ).

Cylindrical concretions represent ancient fluid conduits related to the upward migration of CH_4-rich fluids sourced by gas hydrate destabilisation.

The carbonate–rich rocks of the Tertiary Piedmont Basin stand as one of the first examples of methane-derived rocks that record successive episodes of dissociation and re-formation of gas hydrates and provide precious elements to model the general evolution of a portion of the sedimentary column located within the GHSZ.

Key words: CH_4-derived authigenic carbonates, gas hydrate stability zone, Messinian, Tertiary Piedmont Basin

INTRODUCTION

Interest on gas hydrates has significantly increased in the last decades, due to their potential use as energy source and for their role in climate change and geologic hazard. Gas hydrates are documented worldwide in marine sediments by a wealth of studies carried out with different methodologies. These studies have shown that within the gas hydrate stability zone pure gas hydrates are dispersed in the pore space of marine muds or they concentrate in mm- to some cm-thick, bed parallel layers (e.g. Bohrmann et al., 1998; Suess et al., 1999; Torres et al., 2004; Bohrmann and Torres, 2006). Deeper in the sedimentary column, instead, the reduction of porosity related to sediment compaction prevents their growth within the sediment pore space and force their crystallization in fractures and faults of tectonic origin (e.g. Abegg et al., 2007).

Variations of P and T conditions, related to different processes (sea level drop, tectonic uplift, climate changes, hot fluid rise) induce the destabilisation of gas hydrates, causing the release of huge amounts of gas and water ascending towards the sea floor (e.g. Beauchamp, 2004). Moreover, gas hydrate destabilisation is considered an effective mechanism for triggering large scale marine landslides and sea floor collapses (e.g. Haq, 1993; Paull et al., 1996; Henriet and Mienert, 1998).

Gas hydrate-associated authigenic carbonates have been sampled on present day settings where they form in direct contact with gas hydrates exposed on the sea floor or few meters below it (e.g. Sassen et al., 2004; Mazzini et al., 2006). Two main lithologies have been recognized: a) aragonite crusts, growing within pure gas hydrate layers that are oriented parallel to the bedding surfaces. These carbonates typically show a vacuolar structure that mimics the shape of gas hydrate bubbles (e.g. Bohrmann et al., 1998; Greinert et al. 2001; Teichert et al., 2005); b) monomict breccias, showing no evidence of transportation of the clasts; they are thought to represent collapse breccias, resulting from the rapid destabilisation of gas hydrates formerly present within the sediment pore space (Bohrmann and Torres, 2006). These carbonates, recently defined as clathrites (Bohrmann et al., 2002; Teichert et al., 2005) represent natural archives of the processes responsible for the formation and dissociation of gas hydrates.

In ancient sedimentary sequences exposed onland, many examples of fossil seeps of Proterozoic to Quaternary age have been documented worldwide on the basis of the occurrence of typical authigenic carbonate masses that are recognized for their peculiar fossil content (dense association of chemosymbiotic invertebrates) and their distinctive ^{13}C-depleted isotope values (e.g., Aiello et al., 2001; Kennedy et al., 2001; Aiello, 2005; Campbell, 2006; Campbell et al., 2008). Fluids responsible for their formation were in some cases attributed to destabilisation of gas hydrates on the basis of the characteristic heavy O isotopes in the carbonates (e.g. Clari et al., 2004; Conti et al., 2007; Nyman et al., 2009) or of distinctive sedimentary features (breccias, fractures, soft sediment deformations) related to high gas-fluid flow rate following clathrate destabilisation (Kennett and Fackler-Adams, 2000; Wang et al., 2008).

However, very few examples of carbonate-rich rocks recording the formation of gas hydrates within the sedimentary column, i.e. the evidence of a fossil gas hydrate stability zone, have been documented yet. Notable exception are some Ordovician limestones of Nevada (Krause, 2001), the Oligocene carbonates of the Outer Carpathians (Bojanowski, 2007) and the Mediterranean Neogene dolomitic concretions (Pierre et al., 2002; Pierre and Rouchy, 2004).

In this paper, we describe some carbonate-rich rocks recently discovered in upper Miocene slope sediments of the Tertiary Piedmont Basin that, we propose, represent a solid evidence of the past formation of gas hydrates within the sedimentary column, of their destabilisation, and of the migration of the resulting hydrocarbon-rich fluids toward the sea floor. The study of these rocks provides an opportunity to illustrate the architecture of an ancient gas hydrate stability zone, and to evaluate the processes that acted (and likely act) within this zone.

GEOLOGIC AND STRATIGRAPHIC SETTING

The Tertiary Piedmont Basin (Fig.1), located on the inner side of the Western Alps, is composed of upper Eocene to Messinian sediments deposited unconformably, after the mesoalpine

collisional event, on both alpine metamorphic rocks and Apennine Ligurian units (e.g. Gelati and Gnaccolini, 1988; Mutti et al., 1995; Roure et al., 1996).

The study area is located in the eastern part of the Tertiary Piedmont Basin, south of the Villalvernia-Varzi Line (Fig. 1). This is a E-W striking regional structural feature that was considered as the Alps-Apennine boundary (Elter and Pertusati, 1973). Its main activity took place during the Oligocene-early Miocene interval and was characterized by left-lateral transpressive movements (Di Giulio and Galbiati, 1995; Schumacher and Laubscher, 1996).

The stratigraphic succession here exposed ranges in age from Oligocene to Pliocene and unconformably overlies Ligurian Cretaceous turbidites (Ghibaudo et al., 1985). It is composed of Oligocene continental and fan delta conglomerates followed by upper Oligocene to Middle Miocene basin to shelf terrigenous sediments.

The Upper Miocene part of the succession (Fig. 2), consists of the Sant'Agata Fossili Marls (Tortonian-lower Messinian), the Complesso Caotico della Valle Versa (upper Messinian) and the Conglomerati di Cassano Spinola (upper Messinian).

The Sant'Agata Fossili Marls have been subdivided into two members (Clari and Ghibaudo, 1979):

- the lower member (Tortonian), about 180 m thick, consists of outer shelf sandstones and muddy siltstones (Ghibaudo et al., 1985). At its top, several multiple intraformational discordances**,** corresponding to slump scars, occur (Clari and Ghibaudo, 1979); ellipsoidal, dm-large concretions are hosted in this member.

- the upper member (lower Messinian) is about 100 m thick and consists of slope marls and turbiditic sandstones. In particular, the hemipelagic sediments consist of alternations of burrowed blue-grey silty marls and laminated euxinic mudstones that suggest cyclic variations of oxygen content at the sea bottom (Ghibaudo et al., 1985). In the uppermost part, a lens-shaped conglomerate body, about 500 m wide and 40-50 m thick (S. Alosio Conglomerate), occurs. The particular type of concretions described in this paper have been observed within this muddy member and are clearly different from those found in the lower member (see following).

The vertical evolution from the lower to the upper member of the Sant'Agata Fossili Marls indicates a general deepening of the basin, interpreted to be of tectonic origin. (Ghibaudo et al., 1985).

The Complesso Caotico della Valle Versa (upper Messinian), about 200 m thick, rests, through an erosional surface, on the upper member of the Sant'Agata Fossili Marls and consists of blocks of different composition and size (from meters up to hundreds of meters) floating with a random distribution in a poorly exposed fine-grained matrix (Fig. 2). Most of the blocks are made up of evaporites (swallow tailed selenitic gypsum) deposited during the Mediterranean salinity crisis (e.g. Rouchy and Caruso, 2006). Blocks of authigenic methane-derived carbonates are also present and consist of strongly cemented mud breccias, locally containing remains of chemosymbiotic communities (*Lucina* bivalves and tube worms). This chaotic unit was interpreted as the result of large scale mass wasting events (Dela Pierre et al., 2002; 2007). The occurrence of blocks of methane-derived carbonates indicates, however, the possible contribution of the rise of methane-rich fluids through the sedimentary column in its genesis, as recently suggested for other sectors of the Tertiary Piedmont Basin.

The Conglomerati di Cassano Spinola (upper Messinian), about 400 m thick, consists of lagoonal-lacustrine brackish water deposits, correlatable to the "Lago Mare" interval recognized all over the Mediterranean area (e.g. Orszag Sperber, 2006). They are sharply followed by lower Pliocene open marine muds, that testify the re-establishment of fully marine conditions after the Messinian salinity crisis.

METHODS OF STUDY

Field descriptions of authigenic carbonates, including the geometry and lithology as well as their relationships with the loosely consolidated hosting sediments, have been carried out. Samples of hosting sediments have been collected for biostratigraphic, paleoecologic and stable isotope investigations.

About 100 samples of authigenic carbonates have been selected for petrographic studies and stable isotope analyses.

Petrographic studies were carried out examining 50 standard thin sections by plane polarized and cross polarized light microscopy. Cathodoluminescence observations by a CITL 8220 MK3 equipment have also been done (operating at about 17kV and 400 μA); SEM observations (Cambridge S-360) have been carried out on slightly etched polished surfaces obtained from the same samples used for thin sections (60 stubs).

About 30 sample powders were obtained for C and O stable isotope analyses using a microdrill, in order to separate different portions of rock. The carbonate fraction has been analysed following the classical method (Mc Crea, 1950), in which carbonate powder is reacted in vacuum conditions with 99% orthophosphoric acid at 25°C (time of reaction: 4 hours for calcite and 6 to 7 hours for dolomite). The $^{13}C/^{12}C$ and $^{18}O/^{16}O$ ratios of the CO_2 were obtained using a Finnigan MAT 250 mass spectrometer. For purposes of comparison, a few isotope analyses have also been performed on sediments enclosing the authigenic carbonates. The isotopic ratios are expressed as $\delta^{13}C$ and $\delta^{18}O$ per mil versus the PDB standard; the analytical error is ±0.5‰ and ±0.1‰ for $\delta^{13}C$ and $\delta^{18}O$, respectively.

THE CARBONATE-RICH ROCKS OF RIPA DELLO ZOLFO

Authigenic carbonates have been found in the upper member of the Sant'Agata Fossili Marls and are excellently exposed along a steep escarpment over 150 m high, laterally stretching for about 2 km, known as Ripa dello Zolfo (Sulphur Scarp) because of the occurrence of scattered mm-sized specks of native sulphur. Carbonate-rich rocks occur from the base of the upper member up to 5-6 m below the lower boundary of the overlying Complesso Caotico della Valle Versa (Figs. 2, 3). On the basis of the occurrence of chemosymbiotic macroinvertebrate fossils, mainly consisting of the bivalve *Lucina* sp., two groups have been distinguished: 1) *Lucina*-bearing mud breccias; 2) *Lucina*-free concretions.

Lucina-bearing mud breccias

A single lens-shaped cemented rock body, with a maximum thickness of 6 m and a lateral extent of 15 m, crops out in the lower part of the upper member of Sant'Agata Fossili Marls (Figs. 3, 4A). The boundaries with the hosting loosely consolidated sediments are transitional.

The cemented mass is composed of dark to light grey mud breccias with mm- to cm-sized clasts floating in a fine -grained matrix (Fig. 4B). The clasts are generally rounded and composed of dark muddy siltstones and fine-grained sandstones, belonging to the local Miocene succession. Their fossil content consists of planktonic and benthonic foraminifers, echinoid fragments and bivalve remains. Some clasts are in turn made up of finer-grained mud breccias suggesting the polyphase evolution of the cemented mass. The matrix consists of muddy siltstones and contains both micro and macrofossils (benthic foraminifers, bivalves and gastropods); ovoidal pellets, up to 4 mm in the largest dimension, fill cm-sized cavities and are rimmed by fibrous aragonite. Aragonite also fills the tests of both planktonic and benthonic foraminifers. Finally, pyrite framboids occur within the matrix.

Remains of chemosymbiotic invertebrates are abundant and consist of internal and external molds of *Lucina* bivalves that are preserved both in life position and as disarticulated and fragmented shells (Fig. 4C). Other fossil remains, absent in the hosting sediments occur, such as undetermined mytiloid bivalves and cylindrical structures, 5 mm across, likely referable to tubeworms. Bioturbation is also common and includes both soft and firm ground burrows and borings produced by endholithic bivalves; the boring walls are locally encrusted by a thin rim of aragonite.

A polyphase network of sharp-edged fractures, a mm to a few cm wide, characterizes these rocks. The fractures are arranged sub-perpendicular to bedding and are filled with both internal sediments and carbonate cements. The internal sediments consist of micrite and peloidal-rich micrograinstones of suspect bacterial origin (e.g. Cavagna et al., 1999), and are overlain by a

fibrous aragonite rim (Fig. 4D). Tubular structures, about 10 cm in diameter and showing a central hollow, can be locally observed and likely represent conduits for fluid expulsion.

Lucina-free concretions

This group includes concretions resulting from cementation of the hosting fine-grained sediments and characterized by the lack of remains of chemosymbiotic macroinvertebrates and of evidence of exposure at the sea floor. On the basis of morphologic and lithologic features, two subtypes can be distinguished (Figs. 2, 3): 1) stratiform concretions; 2) cylindrical concretions.

Stratiform concretions

In outcrop, stratiform concretions consist of strongly cemented layers, lying parallel to the bedding surfaces (Fig. 5A). The internal features and degree of complexity allow to further subdivide them in the following categories:

1) Homogeneous concretions

2) Septarian-like cracked concretions

3) Brecciated concretions

Homogeneous concretions

Ten of these concretions have been mapped throughout the upper member of the Sant'Agata Fossili Marls, up to few meters below its upper boundary (Fig. 3). They consist of dm-thick cemented layers with a lateral extent up to 100 meters and are lithologically identical to the enclosing muds except for their strong induration. Petrographic observations indicate that they result from the extensive cementation of the hosting muddy sediments by a microcrystalline dolomite intergranular cement (Fig. 5B). Pyrite crystals and framboids are abundant (Fig. 5C).

In some concretions, sand-sized grains consisting of mica flakes, quartz and rock fragments occur. Some of them are surrounded by a circumgranular pore that may be empty or filled with dolomite cement, up to 0.1 mm thick (Fig. 5D).

Septarian-like cracked concretions

This class includes one instance of three irregularly stacked cemented layers, 10 to 50 cm thick. They crop out in the upper member of the Sant'Agata Fossili Marls, about 20 m below the base of the overlying Complesso Caotico della Valle Versa and are separated by a stratigraphic distance of 2-3 m. The boundaries with the enclosing poorly consolidated sediments are sharp and show a wavy geometry. The lower and the upper layers show a lateral continuity of few meters and a maximum thickness of 20 cm, whereas the middle one can be followed laterally at least for 200 meters, giving rise to a distinct marker bed useful for stratigraphic correlations (Fig. 6A). The following description refers to this latter bed, since it is representative of this class of concretions.

The middle layer consists of grey mudstones and is lithologically identical to homogenous concretion type. Also in this case, the intergranular cement consists of microcrystals of dolomite, ranging in size from a few to 40 μm. Pyrite is abundant but is commonly oxidized. When cut, however, the layer displays an unexpected complexity, due to the occurrence of an intricate network of fractures (Fig. 6B). Most fractures are mm- up to some cm-wide, develop from the central portion of the concretion and gradually thin outward without reaching the outer concretion surface. Their geometry appears to be very similar to septarian cracks that usually are found within dm- to m- sized sub-spherical concretions and form because of contractional processes (e.g. Hendry et al., 2006). In our case, the orientation may be diverse, but generally the cracks lie both perpendicular and parallel to bedding (Fig. 6B). Most fractures are filled either with internal sediments or complex polyphasic carbonate cements. In the upper part of the concretion, however, empty fractures are present, which were never filled (Fig. 6C).

Sediment-fillings consist of dolomite-cemented mudstones; slight textural differences, such as variations in silt-sized quartz and mica grains content, highlight a banding parallel to the crack walls that documents several generations of fracturing and sediment infiltration (Fig. 6D). Commonly, sediment-filled cracks display a microbrecciated structure evidenced by sub-angular to rounded clasts, often fitting to each other, that are elongated parallel to crack walls (Fig. 6D).

Cements, partially or completely filling other cracks (Fig. 7A), consist of sparry dolomite, calcite or Mg-calcite displaying a banding defined by the superposition of more or less turbid layers (Fig. 7B). Cathodoluminescence enables to distinguish different cement zones, follow them, and recognize unusual growth geometries. A first thin isopachous rim of dull yellow to non luminescent to bright yellow dolomite cement fringes the crack walls (Fig. 7C). It is followed by a dull brown to moderate orange zoned calcite cement, with a maximum thickness of several 100's of μm, that does not overgrow uniformly the first dolomite rim. In fact each cement zone tapers out at a point beyond which the following, younger, cement zone directly overlies the first isopachous dolomite rim. In terms of physical stratigraphy, calcite cements pinch out and onlap the substrate. Some segments of the crack system may be even filled completely with the first, dull brown zone of calcite cement, that in the adjacent segment is nearly absent (Fig. 7C).

Brecciated concretions

This class is represented by two coupled layers, 5 m above the septarian-like cracked concretions previously described (Fig. 8A). The layers partially overlap and taper off laterally. They show a lateral extent of 3-4 m and a thickness of 40 cm. Sharp boundaries separate them from the hosting sediments. Internally they are characterized by a brecciated structure, evidenced by mm- to cm-sized clasts with both rounded and angular edges that commonly fit together (Fig. 8B). The clasts are mainly composed of mudstones and siltstones strongly cemented by microcrystals of dolomite. Frequently the same pattern of wedge-shaped fractures, both filled with sediment and cement described in the septarian-like cracked concretions, are preserved in the clasts (Fig. 8C). In

addition, the thin rim of isopachous dolomite cement fringing the cracks in the septarian concretions is also recognizable but only on some sides of some clasts (Figs. 8D). These features suggest that brecciated concretions result from further fracturing of septarian ones. The inter-clast spaces, finally, are filled with white to yellow coarse sparry Mg-calcite cement showing an undulose extinction and a nearly unzoned moderate orange cathodoluminescence color. A high percentage of fluid inclusions makes this cement locally cloudy.

Cylindrical concretions

These concretions occur throughout the upper member of the Sant'Agata Fossili Marls (Figs. 2, 3). Some of them have been observed in the lower part of the unit below the *Lucina*-bearing mud breccias described above; the majority however is concentrated in the upper part of the member, both below and above the stratiform concretions**.**

Cylindrical concretions result from cementation of muddy sediments by microcrystals of dolomite and usually are rich of rusty grains, resulting from oxidation of pyrite. They are very straight and show an equal diameter throughout their length, with long axes perpendicular to bedding (Fig. 8E). They are up to one metre long and 3-70 cm across. In the largest ones an axial portion has been observed (Fig. 8F). It is about 2 cm across, and can be empty or, more commonly, filled with a dark muddy sediment. The boundary between this portion and the walls of the concretions is uneven. Uncompacted burrows can be observed within most of the concretion bodies, suggesting that these features originated from early cementation of sediments deposited under oxygenated conditions.

STABLE ISOTOPE GEOCHEMISTRY

Data

Both the authigenic carbonates and the hosting sediments have been analysed for their C and O stable isotope signature. The results of 34 analyses are reported in Table 1 and summarised in

Fig. 9. The results are confidently representative of the isotopic signature of the authigenic carbonate phases only in those rocks that developed within sediments devoid of a significant pelagic carbonate fraction, such as the *Lucina*-free concretions. On the contrary, in the *Lucina*-bearing mud breccias, an abundant carbonate skeletal fraction (foraminifer tests, nannofossils and a lesser amount of mollusk shells), is present. In this case, the obtained values represent a weighted average of CH_4-derived authigenic intergranular carbonate cement and primary marine carbonate components.

For carbonate filling fractures and voids, sampling methods did not allow to separate cements pertaining to the different precipitation phases evidenced by petrographic and cathodoluminescence analyses. Hence, also in this case the results represent an average of the isotopic content of these different phases

Hosting sediments

The $\delta^{13}C$ ($-4.1 < \delta^{13}C$ ‰ PDB < -1.1) and the $\delta^{18}O$ ($-3.0 < \delta^{18}O$ ‰ PDB < -1.8) values recorded in 4 samples of hosting loosely consolidated marls (Fig. 9) are comparable to those reported in coeval sediments of other Mediterranean sites and are characteristic of formation in open marine conditions (e.g. Bellanca et al., 1986; Pierre and Rouchy, 2004). The moderate ^{13}C depletion is related to a very minor amount of diagenetic carbonate sourced by decaying organic matter, actually very abundant in these sediments and commonly represented by land plant remains.

Lucina- bearing mud breccias

As shown in Fig. 9, the C and O isotopic values of *Lucina*-bearing mud breccias form a well defined cluster. Strongly negative $\delta^{13}C$ values (from -38.4 to -20.7‰ PDB) have been recorded in these rocks, with the maximum ^{13}C depletion in the fracture-filling aragonite. The $\delta^{18}O$ values are significantly positive, ranging from +2.6 up to +4.1 ‰ PDB in all the analyzed samples.

Stratiform concretions

A more widely scattered distribution of C and O isotope values is recognisable in this group (Fig. 9). The $\delta^{13}C$ values of the intergranular dolomite cement of homogeneous and septarian concretion bodies and of the clasts of the brecciated ones range from -59.6 to -13.8 ‰ PDB; the $\delta^{18}O$ values range from +2.7 to +7.9 ‰ PDB, with a single exception of -0.2 ‰ PDB in a clast of a brecciated concretion. A similar range of values has been recorded in the fracture fillings (both primary cements and cemented internal sediments) of septarian and brecciated concretions. In fact the $\delta^{13}C$ values range from -34.4 to -24.7 ‰ PDB whereas the $\delta^{18}O$ from +4.7 to +7.2 ‰ PDB. Only in one sample a less positive value ($\delta^{18}O$ = +1.2 ‰ PDB) has been recorded (Fig. 9). For purposes of comparison, some of the ellipsoidal, dm-sized ordinary concretions occurring within the lower member of the Sant'Agata Fossili Marls have been analyzed and provided $\delta^{18}O$ values close to 0 and $\delta^{13}C$ values around -2 ‰ PDB (S. Cavagna, personal communication, 2009).

Cylindrical concretions

Dolomitic intergranular cement of cylindrical concretions show the typical ^{13}C depletion of the authigenic methane-derived carbonates, with $\delta^{13}C$ ranging from -34.3 to -15.1 ‰ PDB. Oxygen enriched values ($+5.6 < \delta^{18}O$ ‰ PDB $< +7.6$) have been recorded (Fig. 9). No significant differences have been found between the axial part and the walls of the same concretion.

Interpretation

Carbon isotopes

The ^{13}C depletion recorded in all the authigenic carbonate samples points to oxidation of methane as the mechanism responsible for carbonate precipitation in the pores of lower Messinian muds. These depleted values are strictly comparable to those reported in present day (e.g Aloisi et

al., 2000; Han et al., 2004; Reitner et al., 2005; Bahr et al., 2007; Ussler and Paull, 2008) and ancient seep carbonates world-wide (e.g. Peckmann et al. 2002; Campbell et al, 2002; 2008; Clari et al., 1994; 2004; Conti et al., 2008; Himmler et al., 2008). Their high variability (from – 59.6 to – 13.8 ‰ PDB) is related to a mixing of different C pools such as methane of thermogenic and/or biogenic origin, skeletal remains (foraminifers, coccoliths), dissolved inorganic carbon (DIC) in the pore waters, and possibly some isotopically heavy carbon, resulting from local methanogenic processes.

Oxygen isotopes

Most of the $\delta^{18}O$ values range from + 7.8 to + 2.7 ‰ PDB with the exception of two cases concerning the fracture-filling cements of a septarian concretion and the clast of a brecciated one ($\delta^{18}O$ = +1.2 and -0.2 ‰ PDB respectively) (Fig. 9), the correct interpretation of which will require a more accurate microsampling.

The commonly positive $\delta^{18}O$ values suggest that the cements precipitated from fluids enriched in ^{18}O. Different processes can explain such an enrichment: severe evaporation of sea water leading to hypersaline conditions (e.g. McKenzie et al., 1979), dehydration of smectite clay minerals (Dählmann and de Lange, 2003), and gas hydrate destabilisation (e.g. Aloisi et al. 2000; Ussler and Paull, 2001; Pierre and Rouchy, 2004).

The slightly negative oxygen values and the normal marine fossil assemblages of the sediments hosting the concretions exclude the occurrence of evaporitic conditions during deposition of hemipelagic muds. No evidence of subsequent flushing by dense hypersaline waters originated during the Messinian salinity crisis has been found either in the studied section or in coeval sediments of the Tertiary Piedmont Basin.

Both clay mineral dehydratation and gas hydrate destabilisation can instead be taken into account. However, the lack of information about the source of fluids and on clay mineralogy of underlying formations do not allow to discuss the role played by the former mechanism in ^{18}O enrichment. Conversely, the association of positive heavy oxygen values with negative $\delta^{13}C$ ones

supports the hypothesis of gas hydrate destabilisation as the most reliable mechanism sourcing CH_4-rich fluids that at the same time were enriched in ^{18}O and depleted in ^{13}C.

DISCUSSION

Lucina-bearing mud breccias: products of pulsating seepage at the sea floor

The *Lucina*-bearing mud breccias found in the Sant'Agata Fossili Marls may preserve the sea floor product of an ancient seepage site of early Messinian age, as indicated by the occurrence of remains of *Lucina* bivalves. Lucinids are infaunal organisms that live in close proximity (25-50 cm) of the sea floor, at the interface between oxic and anoxic zones, tapping H_2S from the sulfidic zone and maintaining an anterior tube to the surface to supply oxygenated waters (e.g. Taylor and Glover, 2009). Therefore, their occurrence in ancient authigenic methane-derived carbonates is considered a reliable evidence of an origin at the sea floor (e.g. Campbell, 2006).

The compositional and textural features of the cemented sediments suggest that they resulted from a pulsating regime of fluid expulsion, characterized by fast and violent phases alternated with slower and quieter degassing episodes (Clari et al., 2004; Leon et al., 2007). During vigorous seepage, large amounts of overpressured fine-grained sediments, sourced from deeper stratigraphic levels, were extruded at the sea floor, giving rise to the accumulation of mud breccias. Quiet degassing phases were instead responsible for the colonization of the seep sites by chemosymbiotic communities and the local cementation of the extruded sediments. Further episodes of focused fluid flow, resulting from local overpressure created by the formation of a rigid plug in the uppermost meters of the sedimentary column, were responsible for the dismemberment of the already cemented sediments: this is suggested by the occurrence of clasts made up of previously cemented mud breccias and by the occurrence of *Lucina* bivalves not preserved in life position. Overpressured fluids were also responsible for the opening of fractures in the formerly cemented mass, subsequently filled with aragonite splays during further degassing phases.

Finally, when seepage ceased the completely cemented mass was infested by endholithic organisms, as suggested by borings preserved on its outer surface.

Lucina-free concretions: products of gas hydrate formation and dissociation in the subsurface and of the upward migration of the resulting fluids

Stratiform concretions

The bed-parallel geometry of stratiform concretions, their great lateral extension, and their reduced thickness (in the order of decimetres) suggest that carbonate precipitation took place at a geochemical interface parallel to the sea floor.

Isotopic data and the co-occurrence of authigenic carbonate and pyrite suggest that this geochemical front may have corresponded to the sulfate-methane interface (SMI) that develops where methane migrating upward toward the seafloor is progressively oxidised by a consortium of sulfate-reducing bacteria and methanotrophic archea (Boetius et al. 2000). The overall chemical reaction ($CH_4+SO_4^{2-} \rightarrow HCO_3^- + HS^- + H_2O$) produces an increase in alkalinity within the interstitial waters, thus promoting the precipitation of carbonates (e.g. Irwin et al., 1977; Campbell, 2006; Raiswell, 1987; Raiswell and Fischer, 2000, Ussler and Paull, 2008). The dolomite mineralogy of the intergranular cement indicates that concretionary growth occurred within the sediment column (e.g. Rodriguez et al., 2000) just above the SMI, where the concentration of sulfates, that are known to inhibit dolomite precipitation (Baker and Kastner, 1981; Compton, 1988) is very low. This is confirmed by the lack of chemosymbiotic invertebrate communities and other evidences of sea floor exposure.

Thus, the upward flow of CH_4-rich fluids appears to be responsible for the genesis of the simplest type of stratiform concretions, i.e homogeneous concretions

Septarian concretions

Septarian concretions are characterized by a striking internal complexity, due to the occurrence of a network of wedge-shaped fissures that may be empty or filled with either internal sediments or carbonate cements.

The overall geometry of the fissures suggests an origin by shrinkage processes. This is further supported by the common occurrence of dolomite rims around sand-sized terrigenous grains (Fig. 5D), that point to contractional processes at a microscopic scale.

Several mechanisms are reported in literature to explain sediment shrinkage and in particular septarian-cracks:

1) desiccation of clayey sediments; this process can be ruled out because the sediments hosting the concretions were deposited in a slope environment and were permanently submerged.

2) shaking of muddy sediments by synsedimentary earthquakes (Pratt, 2001). No post-depositional sedimentary structures (liquefaction, microfaults) referable to seismic processes have been recognized in coeval surrounding sediments. However, this does not lead to exclude that seismic shocks played a role in the origin of cracks.

3) syneresis. This process is held as responsible for the opening of contractional cracks in smectite-rich muddy sediments, especially where it is enhanced by the decay of bacterial extracellular polysaccharide substances (EPS) binding clay particles (e.g. Dewhurst et al., 1999; Hendry et al,. 2006). Ongoing researches concerning clay mineralogy and biomarker analysis will allow to verify if this last mechanism played a role; however, it seems to be consistent with the flushing of sediments by methane-rich fluids that likely promoted the development of dense microbial communities.

Whatever their origin, the occurrence side by side of sediment-filled, cement-filled and empty fissures, showing the same size and wedge-shaped geometry, indicates that different mechanisms contributed to the filling and the enlargement of primary shrinkage cracks.

Sediment-filled fissures are noteworthy for the internal complexity. The brecciated structure and the alignment of elongated clasts, that fit to each other and to the crack walls, suggest that the

fissures actually correspond to clastic dykes, filled by unconsolidated muddy sediments squeezed from below because of overpressured conditions. The preexisting contractional wedge-shaped fissures provided a network of variably interconnected voids that was exploited by overpressured fluidified muds during their rise through semilithified sediments. Many episodes of forceful mud injection, followed by partial cementation appear to have occurred; every episode both enlarged existing fractures, dismembering the previously injected muds and producing the angular clasts of the breccias, and opened new ones that crosscut hosting sediments and preexisting dykes.

Other fissures are instead filled with carbonate cements. The first phase consists of a finely crystalline variably luminescent dolomite that forms an isopachous rim that fringes all the fissure walls, documenting precipitation in a completely open void. This rim is overlain by zoned calcite cements. The discontinuous and asymmetrical distribution of these cements is contrary to common knowledge about cementation within a water-filled cavity whose walls should be encrusted by more or less regular rims of cement crystals. This unusual pattern may be explained with a process of plugging of the cavity by a solid substance that, some time after formation, started to disappear (Fig. 10). Given the isotopic signature of these rocks, gas hydrates are the best candidates for such a solid. When gas hydrates started to destabilize, new small open spaces began to form after gas hydrate abandonment. Gas-rich fluids, both produced by hydrate dissociation and coming from below, restarted to flow and caused progressive cement precipitation. However, the dissociation of gas hydrates did not proceed uniformly from crack walls toward the centre but in a more irregular way: cements could thus only precipitate in the newly originated voids, resulting in the cement pinch-outs and the very asymmetrical distribution of cement zones (Fig. 10).

Unlike modern carbonates associated to gas hydrates, mainly represented by aragonite, at Ripa dello Zolfo dolomite and calcite are the dominant phases. This discrepancy might be explained considering that the studied features formed in the subsurface, where sulfate-depleted pore waters prevailed. On the contrary, modern examples have been sampled at, or very close to, the sea floor

where sulfate-rich oxygenated sea waters favour aragonite precipitation (e.g Bohrmann and Torres, 2006).

A question arises concerning why some fissures were filled with sediments and others with cements. It is proposed that some contractional fissures were not linked to the main fracture system and thus did not work as conduits for sediment-entraining overpressured fluids. These fissures were sealed by gas hydrates, thus preventing sediment injection. In this case, it may be suggested that growth of clathrates also caused enlargement of smaller pristine shrinkage cracks as a result of volume expansion. These fissures, therefore, would record two distinct phases of gas hydrate formation and dissociation, the first being responsible for cavity enlargement, the second for discontinuous calcite cement precipitation. These two phases are separated by precipitation of the isopachous dolomite rim that fringed the walls of open cavities.

A last question relates to the occurrence of still empty fissures. We envisage that this feature is related to the inhomogeneous distribution of gas hydrates in the sedimentary column, as frequently reported in present day settings (e.g. Beauchamp, 2004; Ussler and Paull, 2008). In particular, it is proposed that while some fissures were being filled with pinchout calcite cements as a consequence of the localized destabilisation of gas hydrates, other fissures could not record this cementation phase because they were still sealed by gas hydrates and no space was available for carbonate cements. Later on, when gas hydrates fully disappeared, carbonate precipitation could not take place, because of inhibition of anaerobic oxidation of methane resulting from the absence, in the pore waters, of sulfate ions: the latters were in fact previously consumed by rapid precipitation of zoned calcite cements in adjacent fractures. In this regard, it is worth noting that observations on present day settings have shown that anaerobic oxidation of methane proceeds at very fast rates and large amounts of authigenic carbonates can form on the time scale of centuries to millennia (e.g. Ussler and Paull, 2008). Because of exhaustion of sulfates, the SMI was rapidly displaced upwards, anaerobic oxidation of methane was inhibited and no carbonate cements could precipitate in the fractures lastly abandoned by gas hydrates.

Brecciated concretions

The features of the clasts of brecciated concretions indicate that they formed through the fracturing of septarian cracked ones. The jigsaw puzzle pattern of the clasts, the lack of any evidence of transport and the stratal geometry of the concretions suggest that brecciation was produced *in situ* and was not the result of hydraulic fracturation related to channelled overpressured fluids violently ascending towards the basin floor. The occurrence of thin dolomite rims on only some sides of the clasts indicates that fracturing followed dolomite lining of septarian-like cracks. It is suggested that, in this case, volume expansion resulting from the growth of gas hydrates in the previously formed cracks was responsible for the formation of a gas hydrate-cemented breccia. Since the density of gas hydrates is 0,910g/cm^3 (Sloan, 1998), their crystallisation promotes in fact a significant volume expansion leading to sediment deformation through a frost heave mechanism (e.g. Krause, 2001). When gas hydrates started to decompose, the collapse of clasts occurred, followed by precipitation of Mg-calcite spar. The absence of growth asymmetries and pinch outs documents that this cement did not precipitate along with gas hydrate destabilisation but when the latter had completely disappeared.

Cylindrical concretions

Cylindrical concretions, reported both on present day sea bottoms (Orpin, 1997; Stakes et al., 1999; Diaz del Rio et al., 2003; Takeuchi et al., 2007) and in the fossil record (Aiello et al., 2001; Aiello, 2005; Pierre et al., 2002; Mazzini et al., 2003; Clari et al., 2004; Pierre and Rouchy, 2004; De Boever et al., 2006; Nyman et al., 2009) represent ancient fluid conduits related to the upward migration of CH_4-rich fluids sourced, in the case under study, by the destabilisation of gas hydrates. The precipitation of microcrystalline dolomite cement took place in the pores of the terrigenous sediments along the conduits and was caused by microbial degradation of methane, coupled with sulfate reduction, suggested by the presence of pyrite, in a portion of sedimentary

column comprised between the SMI and the sea floor. The axial portion of the concretions corresponds to the central channel of the conduit that was filled with sediments only when the active flux ceased (Clari et al., 2004; Nyman et al., 2009).

Depth of formation of *Lucina*-free concretions

Different lines of evidences indicate that *Lucina*-free concretions originated at an early diagenetic stage, at shallow burial depth:

1) the occurrence in some concretions (cylindrical, septarian-cracked) of uncompacted burrows, suggesting that sediments did not suffer a significant volume reduction before cementation took place;

2) the presence of shrinkage-related structures that implies that the original high pore volume of mudstones had not been significantly reduced when concretion growth took place;

3) the precipitation of the intergranular cement at the SMI, whose depth in present day settings ranges from few dm up to few tens of m (e.g. Rodriguez et al., 2000; Takeuchi et al., 2007).

Conditions for gas hydrate formation

In order to check the possibility that gas hydrates could form and be stable in the Tertiary Piedmont Basin during the early Messinian, the phase diagram of gas hydrates in marine sediments (Kvenvolden, 1998; Bohrmann and Torres, 2006) has been applied to the Sant'Agata Fossili Marls. (Fig. 11A). Depth of deposition, temperature, salinity of the water column and the geothermal gradient have been considered, assuming methane as the trapped gas.

Sedimentologic and micropaleontologic data indicate that the Sant'Agata Fossili Marls were deposited in a slope environment in the medium-lower bathyal zone, i.e. between -500 and –1000 m below sea level (Ghibaudo et al., 1985; E. Bicchi 2008, personal communication). Normal salinity conditions, revealed by the common occurrence of remains of stenohaline organisms (i.e. echinoid fragments and spines), and a geothermal gradient of 30 °C/km, have been considered (e.g.

Mosca, 2006). A surface water temperature of 18°C has been used, on the basis of recent paleoclimatic interpretations of the late Tortonian-early Messinian time interval (Bosellini and Perrin, 2008). Applying this latter value to a typical ocean profile, sea floor temperatures of 7°C and 4°C have been obtained for depths of deposition of 500 and 1000 m respectively (Fig.11A) .

The resulting stability fields (Fig.11B) show that gas hydrates could indeed be stable within the lower Messinian sediments of the Tertiary Piedmont Basin: at a water depth of 500 m the thickness of the gas hydrate stability zone would be of few tens of metres, whereas at 1000 m it could attain a maximum thickness of 400 m.

Source of methane

The strong depletion of ^{13}C recorded in most of the concretions (with $\delta^{13}C$ values as low as -59‰ PDB) suggests that hydrocarbons were generated by biogenic microbial methanogenesis. In this light, the abundant land plant debris observed in the Sant'Agata Fossili Marls could be regarded as possible source for biogenic methane. However, a deep thermogenic source, located in the Mesozoic sequence that underlies the local Cenozoic succession, cannot be ruled out and would account for the less depleted C isotope values recorded in some concretions. In this light, the Villalvernia-Varzi Line, a strike-slip fault of regional importance that bounds to the North the Ripa dello Zolfo area, and the related fracture system, could have worked as a preferential pathway for the upward flow of deep-seated fluids.

AN ANCIENT GAS HYDRATE STABILITY ZONE PRESERVED IN THE SANT'AGATA FOSSILI MARLS ?

The wide array of carbonate rich-rocks hosted in the lower Messinian sediments of Ripa dello Zolfo provides evidence of the formation of gas hydrate in the sedimentary column, of their dissociation at different rates, and of the upward migration of the resulting hydrocarbon-rich fluids toward the

sea bottom. These phenomena are widely documented in present day settings but poorly recognized in the geologic record.

The stratigraphic relationships among different types of authigenic carbonates indicate that two main episodes of methane flow occurred. During the first one the fluids, delivered by destabilisation of gas hydrate hosted at deeper stratigraphic levels, reached the sea floor giving rise to the *Lucina*-bearing mud breccias enclosed in the lower part of the studied section (Fig. 12A). The ascending fluid pathways are represented by cylindrical concretions located below the mud breccias. The second episode is testified by stratiform and cylindrical concretions located in the upper part of the section, above the mud breccias (Fig. 12B).

Size, geometry, isotope composition, and internal features of stratiform concretions clearly differentiate them from ordinary dm-sized ellipsoidal concretions commonly found within organic-rich muddy sediments and actually present in the lower member of the Sant'Agata Fossili Marls. In particular, the strict association of stratiform concretions with undisputable seep carbonates (*Lucina* -bearing mud breccias) and cemented gas conduits (cylindrical concretions) and the occurrence of clastic dykes, document that their genesis is not related simply to local degradation of organic matter but to an upward advection of methane-rich fluids originated deeper in the sedimentary column. Some of these concretions show unusual internal structures (zoned calcite cements) that may be related to the past occurrence of hydrates in the sediments. Thus, these concretions mark a portion of the sedimentary column located within a (paleo) gas hydrate stability zone (GHSZ).

At Ripa dello Zolfo, preservation of the vestiges of the former presence of hydrates within the sediments is assured by a network of secondary fissures, mainly due to syneresis-driven shrinkage processes, in which the diagenetic products related to the formation and destabilisation of gas hydrates are retained.

The following step by step evolution of stratiform concretions can be sketched, based on the reconstruction and correlation of the complex sequence of diagenetic events recognized within them (Fig. 13):

1) sedimentation of silty clays in a slope environment.

2) Diffuse flow of CH_4 -rich fluids, anoxic oxidation of methane and precipitation of a pervasive intergranular dolomite cement along the SMI, few meters below the sea floor, giving origin to homogeneous concretions (Fig. 13A). This process affected repeatedly distinct levels of the sedimentary column, as suggested by the occurrence of several superposed cemented layers. In some of these beds a network of secondary fissures was further generated by shrinkage processes (Fig. 13A).

3) Enlargement of secondary fissures (Fig. 13B) by: a) repeated episodes of forceful injection of overpressured sediments; b) frost-heave mechanisms related to gas hydrate crystallisation. This implies that only a part of the fissures were occupied by gas hydrates, the others forming a network along which sediment-rich fluids flowed upward, together with free gas that sustained the stability of hydrates.

4) Upward migration of the base of the GHSZ and consequent destabilisation of gas hydrates leading to precipitation of dolomite, both as intergranular cement of clastic dykes and as an isopachous rim fringing the walls of the fissures previously occupied by gas hydrates (Fig. 13C).

5) New phase of crystallisation of gas hydrates in the open cracks. At shallow burial depth, volume expansion related to gas hydrate growth could further enlarge the cracks and fracture the partially lithified sediments, thus producing a gas hydrate-cemented breccia. Deeper in the sedimentary column, gas hydrates could not expand, because of the greater lithostatic load, and simply plugged the cracks (Fig. 13D) .

6) Progressive upward displacement of the GHSZ base. At deeper burial depths, the localized destabilisation of gas hydrates and the concomitant precipitation of cements gave rise to the pinch out cements observed in some fissures of the septarian concretions. In other fissures and in overlying sediments, gas hydrates were instead still stable (Fig. 13E).

7) A further upward shift of the GHSZ base induced the dissociation of clathrates also at shallower depths, resulting in the formation of collapse breccias. Continuous flux of CH_4-rich fluids promoted

the precipitation of sparry Mg-calcite cements in the interclast spaces, thus generating the brecciated concretions (Fig. 13F). Deeper in the sediment column, carbonate precipitation could not take place because of unsuitable geochemical conditions, and part of the fissures of the septarian concretions remained empty.

The ascending pathways of the fluids in the subsurface are documented by the cylindrical concretions, that have been recognized throughout all the studied section.

The scenario depicted above suggests that the GHSZ in the Late Miocene in this area was highly dynamic and was shifting up and down so that the studied portion of sedimentary column could record different phases of formation and destabilisation of gas hydrates. Both local and regional factors could indeed affect stability of gas hydrates:

1) the close proximity of the Ripa dello Zolfo to a strike-slip fault of regional importance such as the Villalvernia-Varzi Line. The intermittent activity of this structure, providing a fracture system for fluid migration, could in fact favour the pulsating expulsion of deep-seated methane-rich fluids. This interpretation is supported by observations on modern sea floors, where the strict association among strike-slip and transform faults, methane venting, gas hydrate destabilisation and authigenic carbonate formation is widely documented (e.g. Paull et al., 2007).

2) Temperature and relative sea level changes heralding the Messinian salinity crisis (e.g. Ryan, 2009) that could actively influence the stability of gas hydrates in the studied sediments that, as already said, formed at a very shallow burial depth.

CONCLUSIONS

The Ripa dello Zolfo carbonate-rich rocks are a solid evidence of the fossil counterpart of a GHSZ. The exceptional preservation in the fossil record of the formation of gas hydrates within the sedimentary column is the result of the combination of two factors: 1) the development of a network of wide secondary fissures, in which gas hydrates could grow; 2) the precipitation of authigenic carbonates both within the intergranular pores of muddy sediments, that hindered

obliteration of these features by burial compaction, and as fissure-filling cements that show diagnostic criteria to infer the formation and destabilisation of gas hydrates.

Carbonate precipitation was controlled by the relative position of the base of the GHSZ, guiding in turn the upward methane flux, and of the SMI, i.e. the chemical interface above which methane oxidation and sulfate reduction take place simultaneously, resulting in a marked increase in alkalinity. The vertical movements of both these surfaces depend on different and independent factors such as rate of gas-charged upward fluid flow, and downward advection of sulfate-rich waters bathymetry and temperature of sea water.

The studied authigenic carbonates stand as a rare example of fossil clathrites. However, they differ from present-day ones because they formed within the sediment column, at a depth where geochemistry of pore fluids favoured precipitation of dolomite/calcite instead of aragonite, that is ubiquitous on modern sea floors.

The Ripa dello Zolfo features provide an opportunity to unravel the evolution both in space and time of a portion of the sedimentary column located within the GHSZ, and show that the distribution of gas hydrates was inhomogeneous both in space and in time. At any given moment, only a part of the pores were occupied by gas hydrates, the others forming a network along which free gas flowed upward and sustained the stability of hydrates. Moreover, the base of the GHSZ in time moved up and down in the sedimentary column and a given stratigraphic level experienced successive episodes of dissociation and re-formation of gas hydrates in a short time interval. This confirms observations on present day GHSZ, where vertical gas migration actually occurs and gas hydrate are continuously forming and dissociating (e.g. Hovland and Svensen, 2006; Liu and Flemings, 2006; Paull et al. 2008).

ACKNOWLEDGEMENTS

The authors would like to thank S. Cavagna and A. Festa for their assistance in the field and E. Bicchi for micropaleontologic analyses. S. Cavagna is also thanked for the help in stable isotope

and SEM analyses. Advice and criticisms of Christian Koeberl, Ken MacLeod and two anonymous reviewers substantially improved the paper. Research was funded by MIUR (grants to P. Clari) and CNR, Istituto di Geoscienze e Georisorse, Torino.

REFERENCES

Abegg, F., Bohrmann, G., Freitag, J., and Kuhs, W., 2007, Fabric of gas hydrate in sediments from Hydrate Ridge- results from ODP Leg 204 samples: Geo-Marine Letters, v. 27, p. 269-277.

Aiello, I. W., 2005, Fossil seep structures of the Monterey Bay region and tectonic/structural controls on fluid flow in an active transform margin: Palaeogeography Palaeoclimatology Palaeoecology, v. 227, p. 124-142.

Aiello, I. W., Garrison, R. E., Moore, J. C., Kastner, M., and Stakes, D. S., 2001, Anatomy and origin of carbonate structures in a Miocene cold-seep field: Geology, v. 29, p. 1111-1114.

Aloisi, G., Pierre, C., Rouchy, J. M., Foucher, J. P., Woodside, J., and Party, M. S., 2000, Methane-related authigenic carbonates of eastern Mediterranean Sea mud volcanoes and their possible relation to gas hydrate destabilisation: Earth and Planetary Science Letters, v. 184, p. 321-338.

Bahr, A., Pape, T., Bohrmann, G., Mazzini, A., Haeckel, M., Reitz, A., and Ivanov, M., 2007, Authigenic carbonate precipitates from NE Black Sea: a mineralogical, geochemical, and lipid biomarker study: International Journal of Earth Sciences, (DOI. 10.1007/s00531-007-0264-1).

Baker, P. and Kastner, M., 1981, Constraints on the formation of sedimentary dolomite: Science, v. 213, p. 214-216.

Beauchamp, B., 2004, Natural gas hydrates: myths, facts and issues: Comptes Rendus Geoscience, v. 336, p. 751-765.

Bellanca, A., Calderone, S., and Neri, R., 1986, Isotope geochemistry, petrology and depositional environments of the diatomite-dominated Tripoli Formation (Lower Messinian), Sicily: Sedimentology, v. 33, p. 729-743.

Bigi G., Cosentino D., Parotto M., Sartori R. and Scandone P. (1990) – Structural model of Italy: Geodinamic project. C.N.R., S.EL.CA, scala 1:500.000, Foglio 1.

Boetius, A., Ravenschlag, K., Schubert, C. J., Rickert, D., Widdel, F., Gieseke, A., Amann, R., Jorgensen, B. B., Witte, U., and Pfannkuche, O., 2000, A marine microbial consortium apparently mediating anaerobic oxidation of methane: Nature, v. 407, no. 6804, p. 623-626.

Bohrmann, G. and Torres, M.E., 2006, Gas hydrates in marine sediments, In: Schulz, H.D.and Zabel, M. (Eds.), Marine geochemistry, Springer, pp. 481-512.

Bohrmann, G., Greinert, J., Suess, E., and Torres, 1998, Authigenic carbonates from the Cascadia subduction zone and their relation to gas hydrates stability: Geology, v. 26, p. 647-650.

Bohrmann, G., Suess, E., Greinert, J., Teichert, B., and Naehr, T., 2002, Gas hydrate carbonates from Hydrate ridge, Cascadia convergent margin: indicators of near-seafloor clathrate deposits, In Proceedings of the Fourth International Conference on Gas Hydrates, Yokohama, Japan, p. 102-107.

Bojanowski, M. J., 2007, Oligocene cold-seep carbonates from the Carpathians and their inferred relation to gas hydrates: Facies, v. 53, p. 347-360.

Borowski, W. S., Paull, C. K., and Ussler, W., 1999, Global and local variations of interstitial sulfate gradients in deep-water, continental margin sediments: Sensitivity to underlying methane and gas hydrates: Marine Geology, v. 159, p. 131-154.

Bosellini, F. R., and Perrin, C., 2008, Estimating Mediterranean Oligocene-Miocene sea-surface temperatures: An approach based on coral taxonomic richness: Palaeogeography Palaeoclimatology Palaeoecology, v. 258, p. 71-88.

Campbell, K. A., 2006, Hydrocarbon seep and hydrothermal vent paleoenvironments and paleontology: Past developments and future research directions: Palaeogeography Palaeoclimatology Palaeoecology, v. 232, p. 362-407.

Campbell, K. A., Farmer, J. D., and Des Marais, D., 2002, Ancient hydrocarbon seeps from the Mesozoic convergent margin of California: carbonate geochemistry, fluids and palaeoenvironments: Geofluids, v. 2, p. 63-94.

Campbell, K.A, Francis, D.A., Collins, M., Gregory, M.R., Nelson, C.S., Greinert, J. and Aharon, P., 2008, Hydrocarbon-seep carbonates of a Miocene forearc (East Coast Basin), North Island, New Zealand: Sedimentary Geology, v. 204, p. 83-105.

Cavagna, S., Clari, P., and Martire, L., 1999, The role of bacteria in the formation of cold seep carbonates: geological evidence from Monferrato (Tertiary, NW Italy): Sedimentary Geology, v. 126, p. 253-270.

Clari, P., and Ghibaudo, G., 1979, Multiple slump scars in the Tortonian type area – Piemont Basin, North-Western Italy: Sedimentology, v. 26, p. 719-730.

Clari, P., Fornara, L., Ricci, B., and Zuppi, G. M., 1994, Methane-derived carbonates and chemosymbiotic communities of Piedmont (Miocene, Northern Italy) - an update: Geo-Marine Letters: v. 14, p. 201-209.

Clari, P., Cavagna, S., Martire, L., and Hunziker, J., 2004, A Miocene mud volcano and its plumbing system: A chaotic complex revisited (Monferrato, NW Italy): Journal of Sedimentary Research: v. 74, p. 662-676.

Compton, J.S., 1988, Degree of supersaturation and precipitation of organogenic dolomite: Geology: v. 16, 318-321.

Conti, S., Artoni, A., and Piola, G., 2007, Seep-carbonates in a thrust-related anticline at the leading edge of an orogenic wedge: The case of the middle-late Miocene Salsomaggiore Ridge (Northern Apennines, Italy): Sedimentary Geology, v. 199, p. 233-251.

Conti, S., Fontana, D., and Lucente, C. C., 2008, Authigenic seep-carbonates cementing coarse-grained deposits in a fan-delta depositional system (middle Miocene, Marnoso-arenacea Formation, central Italy): Sedimentology, v. 55, p. 471-486.

Dählmann, A., and de Lange, G. J., 2003, Fluid-sediment interactions at Eastern Mediterranean mud volcanoes: a stable isotope study from ODP Leg 160: Earth and Planetary Science Letters, v. 212, p. 377-391.

De Boever, E., Swennen, R., and Dimitrov, L., 2006, Lower Eocene carbonate cemented chimneys (Varna, NE Bulgaria): Formation mechanisms and the (a)biological mediation of chimney growth?: Sedimentary Geology, v. 185, p. 159-173.

Dela Pierre, F., Clari, P., Cavagna, S., and Bicchi, E., 2002, The Parona chaotic complex: a puzzling record of the Messinian (Late Miocene) events in Monferrato (NW Italy): Sedimentary Geology, v. 152, p. 289-311.

Dela Pierre, F., Festa, A., and Irace, A., 2007, Interaction of tectonic, sedimentary, and diapiric processes in the origin of chaotic sediments: An example from the Messinian of Torino Hill (Tertiary Piedmont Basin, northwestern Italy): Geological Society of America Bulletin, v. 119, p. 1107-1119.

Dewhurst, D.N., Cartwright, J.A. and Lonergan, L., 1999, The development of polygonal fault systems by syneresis of colloidal sediments: Marine and Petroleum Geology, v. 16, p. 793-810.

Diaz-del-Rio, V., Somoza, L., Martinez-Frias, J., Mata, M. P., Delgado, A., Hernandez-Molina, F. J., Lunar, R., Martin-Rubi, J. A., Maestro, A., Fernandez-Puga, M. C., Leon, R., Llave, E., Medialdea, T., and Vazquez, J. T., 2003, Vast fields of hydrocarbon-derived carbonate chimneys related to the accretionary wedge/olistostrome of the Gulf of Cadiz: Marine Geology, v. 195, p. 177-200.

Di Giulio, A., and Galbiati, B., 1995, Interaction between tectonics and deposition into an episutural basin in the Alps-Apennine knot, In Polino, R., and Sacchi, R. (Eds.), Atti del Convegno Rapporti Alpi-Appennino: Accademia Nazionale delle Scienze detta dei XL, Scritti e Documenti, v. 14, p. 113-128.

Elter, P. and Pertusati, P. (1973), Considerazioni sul limite Alpi-Appennino e sulle relazioni con l'arco delle Alpi occidentali: Memorie della Società Geologica Italiana, v. 12, p. 359-375.

Gelati, R., and Gnaccolini, M., 1988, Sequenze deposizionali in un bacino episuturale, nella zona di raccordo tra Alpi ed Appennino settentrionale: Atti Ticinesi di Scienze della Terra, v. 31, p. 340-350.

Ghibaudo, G., Clari, P. and Perello, M., 1985, Litostratigrafia, sedimentologia ed evoluzione tettonico-sedimentaria dei depositi miocenici del margine Sud- Orientale del Bacino Terziario Ligure-Piemontese (Valli Borbera, Scrivia e Lemme): Bollettino della Società Geologica Italiana., v. 104, p. 349-397.

Greinert, J., Bohrmann, G., and Suess, E., 2001, Gas hydrates-associated carbonates and methane venting at Hydrates Ridge: classification, distribution, and origin of authigenic lithologies: Natural Gas Hydrates: Occurrence, distribution and detection. Geophysical monograph, v. 124, p. 99-113.

Han, X. Q., Suess, E., Sahling, H., and Wallmann, K., 2004, Fluid venting activity on the Costa Rica margin: new results from authigenic carbonates: International Journal of Earth Sciences, v. 93, p. 596-611.

Haq, B.U., 1993, Deep-sea response to eustatic change and significance of gas hydrates for continental margin stratigraphy: International Association of Sedimentologists, Special Publication, v. 18**,** p. 93-106.

Hendry, J. P., Pearson, M. J., Trewin, N. H., and Fallick, A. E., 2006, Jurassic septarian concretions from NW Scotland record interdependent bacterial, physical and chemical processes of marine mudrock diagenesis: Sedimentology, v. 53, p. 537-565.

Henriet, J. P., and Meniert, J., 1998, Gas hydrates: relevance to world margin stability and climatic changes: Geological Society, Special Publication, v. 137, p. 1-338.

Himmler, T, Freiwald, A., Stollhofen, H., and Peckmann, J., 2008, Late Carboniferous hydrocarbon-seep carbonates from the glaciomarine Dwyka Group, southern Namibia: Palaeogeography Palaeoclimatology Palaeoecology, v. 257, p. 185-197.

Hovland, M., and Svensen, H., 2006, Submarine pingoes: Indicators of shallow gas hydrates in a pockmark at Nyegga, Norwegian Sea: Marine Geology, v. 228, p. 15-23.

Irwin, H., Curtis, C., and Coleman, M., 1977, Isotopic evidence for source of diagenetic carbonates formed during burial of organic rich sediments: Nature, v. 269, p. 209-213.

Kennedy, M.J., Christie –Blick, N., and Sohl, L.E., 2001, Are Proterozoic cap carbonates and isotopic excursions a record of gas hydrate destabilization following Earth's coldest intervals ?: Geology, v. 29, p. 443-446.

Kennett, J.P., and Fackler-Adams, B.N., 2000, Relationship of clathrate instability to sediment deformation in the upper Neogene of California: Geology, v. 28, p. 215-218.

Krause, F. F., 2001, Genesis and geometry of the Meiklejohn Peak lime mud-mound, Bare Mountain Quadrangle, Nevada, USA: Ordovician limestone with submarine frost heave structures-a possible response to gas clathrate hydrate evolution: Sedimentary Geology, v. 145, p. 189-213.

Kvenvolden, K., A., 1998, A primer on the geological occurrence of gas hydrate: In: Henriet, J. P., and Meniert, J., 1998, Gas hydrates: relevance to world margin stability and climatic changes: Geological Society, Special Publication, v. 137, p. 9-30.

Leon, R., Somoza, L., Medialdea, T., Gonzalez, F. J., Diaz-del-Rio, V., Fernandez-Puga, M. C., Maestro, A., and Mata, M. P., 2007, Sea-floor features related to hydrocarbon seeps in deepwater carbonate-mud mounds of the Gulf of Cadiz: from mud flows to carbonate precipitates: Geo-Marine Letters, v. 27, p. 237-247.

Liu, X. and Flemings, P.B., 2006, Passing gas through the hydrate stability zone at southern Hydrate Ridge, offshore Oregon: Earth and Planetary Science Letters, v. 241, p. 211-226.

Mazzini, A., Jonk, R., Duranti, D., Parnell, J., Cronin, B., and Hurst, A., 2003, Fluid escape from reservoirs: implications from cold seeps, fractures and injected sands - Part I. The fluid flow system: Journal of Geochemical Exploration, v. 78-9, p. 293-296.

Mazzini, A., Svensen, H., Hovland, M., and Planke, S., 2006, Comparison and implications from strikingly different authigenic carbonates in a Nyegga complex pockmark, G11, Norvegian Sea: Marine Geology, v. 231, p. 89-102.

Mc Crea, J. M., 1950, The isotopic chemistry of carbonates and a paleotemperature scale: Journal of Chemical Physics, v. 18, p. 849.

McKenzie, J. A., Jenkyns, H. C., and Bennet, G. G., 1979, Stable isotope study of the cyclic diatomite-claystones from the Tripoli Formation, Sicily: a prelude to the Messinian Salinity crisis: Palaeogeography, Palaeoclimatology, Palaeoecology, v. 29, p. 125-141.

Mosca, P., 2006, Neogene basin evolution in the Western Po Plain (NW Italy): insights from seismic interpretations, subsidence analysis and low (U-Th)/He thermochronology: [Ph.D.thesis]: Amsterdam, The Netherlands, Vrije University, p. 167.

Mutti, E., Papani, L., Di Biase, D., Davoli, G., Segadelli, S., and Tinterri, R., 1995, Il Bacino Terziario Epimesoalpino e le sue implicazioni sui rapporti Alpi-Appennino: Memorie di Scienze Geologiche, v. 47, 217-244.

Nyman, S.L., Nelson, C.S., and Campbell, K.A., 2009, Miocene tubular concretions in East Coast Basin, New Zealand: analogue for the subsurface plumbing of cold seeps: Marine Geology, doi:10.1016/j.margeo.2009.03.021.

Orpin. A.R., 1997, Dolomite chimneys as possible evidence of coastal fluid expulsion, uppermost Otago continental slope, southern New Zealand: Marine Geology, v. 138, p. 51-67.

Orszag-Sperber, F., 2006, Changing perspectives in the concept of "Lago-Mare" in Mediterranean Late Miocene evolution: Sedimentary Geology, v. 188, p. 259-277.

Paull, C. K., Buelow, W. J., Ussler, W., and Borowski, W. S., 1996, Increased continental-margin slumping frequency during sea-level lowstands above gas hydrate-bearing sediments: Geology, v. 24, p. 143-146.

Paull, C.K., Ussler, W., III., Peltzer, E., Brewer, P., Keaten, R., Mitts, P., Nealon, J., Greinert, J., Herguera, J.-C., and Perez, E., 2007, Authigenic carbon entombed in methane-soaked sediments from the northeastern transform margin of the Guaymas Basin, Gulf of California: Deep Sea Research II, vol. 54, p. 1240-1267.

Paull, C. K., Normark, W. R., Ussler, W., Caress, D. W., and Keaten, R., 2008, Association among active seafloor deformation, mound formation, and gas hydrate growth and accumulation within the seafloor of the Santa Monica Basin, offshore California: Marine Geology, v. 250, p. 258-275.

Peckmann, J., Goedert, J. L., Thiel, V., Michaelis, W., and Reitner, J., 2002, A comprehensive approach to the study of methane-seep deposits from the Lincoln Creek Formation, western Washington State, USA: Sedimentology, v. 49, p. 855-873.

Pierre, C., and Rouchy, J. M., 2004, Isotopic compositions of diagenetic dolomites in the Tortonian marls of the western Mediterranean margins: evidence of past gas hydrate formation and dissociation: Chemical Geology, v. 205, p. 469-484.

Pierre, C., Rouchy, J. M., and Blanc-Valleron, M. M., 2002, Gas hydrate dissociation in the Lorca Basin (SE Spain) during the Mediterranean Messinian salinity crisis: Sedimentary Geology, v. 147, p. 247-252.

Pratt, B. R., 2001, Septarian concretions: internal cracking caused by synsedimentary earthquakes: Sedimentology: v. 48, p. 189-213.

Raiswell, R., 1987, Non- steady state microbial diagenesis and the origin of carbonate concretion and nodular limestones: In Marshall, J.D. (Ed.), Diagenesis of sedimentary sequences, Geological Society, London, Special Publication, v. 36, p. 41-54.

Raiswell, R., and Fisher, Q.J., 2000, Mudrock-hosted concretions: a review of growth mechanisms and their influence on chemical and isotopic composition: Journal of the Geological Society, London, v. 157, p. 239-251.

Rodriguez, N.M., Paull, C.K., and Borowski, W.S., 2000, Zonation of authigenic carbonates within gas hydrate–bearing sedimentary sections on the Blake Ridge: offshore southeastern North

America: In: Paull, C.K., Matsumoto, R., Wallace, P.J., and Dillon, W.P. (Eds.), Proceeding Ocean Drilling Project, Scientific Results, vol. 164: College Station, TX (Ocean Drilling Program), p. 301–312.

Reitner, J., Peckmann, J., Reimer, A., Schumann, G., and Thiel, V., 2005, Methane-derived carbonate build-ups and associated microbial communities at cold seeps on the lower Crimean shelf (Black Sea): Facies, v. 51, p. 71-84.

Rouchy, J. M., and Caruso, A., 2006, The Messinian salinity crisis in the Mediterranean basin: A reassessment of the data and an integrated scenario: Sedimentary Geology, v. 188, p. 35-67.

Roure, F., Bergerat, F., Damotte, B., Mugnier, J.L., and Polino, R., 1996, The Ecors-Crop Alpine seismic traverse: Bullettin Societé Géologique de France, n.s. 170, p 1-113.

Ryan, W.B.F., 2009, Decoding the Mediterranean salinity crisis: Sedimentology, v. 56, p. 95-136.

Sassen, R., Roberts, H. H., Carney, R., Milkov, A. V., DeFreitas, D. A., Lanoil, B., and Zhang, C. L., 2004, Free hydrocarbon gas, gas hydrate, and authigenic minerals in chemosynthetic communities of the northern Gulf of Mexico continental slope: relation to microbial processes: Chemical Geology, v. 205, p. 195-217.

Schumacher, M. E., and Laubscher, H. P., 1996, 3D crustal architecture of the Alps-Apennines join - A new view on seismic data: Tectonophysics, v. 260, p. 349-363.

Sloan, E.D. Jr., 1998, Physical/chemical properties of gas hydrates and their application to world margin instability and climatic change. In: Henriet, J. P., and Meniert, J., 1998, Gas hydrates: relevance to world margin stability and climatic changes: Geological Society, Special Publication, v. 137, p. 31-50.

Stakes, D. S., Orange, D., Paduan, J. B., Salamy, K. A., and Maher, N., 1999, Cold-seeps and authigenic carbonate formation in Monterey Bay, California: Marine Geology, v. 159, p. 93-109.

Suess, E., Torres, M.E., Bohrmann, G., Collier, R.W., Greinert, J., Linke, P., Rehder, G., Trehu, A.M., Wallmann, K., Winckler, G. and Zuleger, E., 1999, Gas hydrate destabilisation: enhanced

dewatering, benthic material turnover and large methane plumes at the Cascadia convergent margin: Earth and Planetary Science Letters, v. 170, p. 1-15.

Takeuchi, R., Matsumoto, R., Ogihara, S., and Machlyama, H., 2007, Methane-induced dolomite "chimneys" on the Kuroshima Knoll, Ryukyu Islands, Japan: Journal of Geochemical Exploration, v. 95, p. 16-28.

Taylor, J.D., and Glover, E.A., 2009, A giant Lucinid bivalve from the Eocene of Jamaica – Systematica, life habits and chemosymbiosis (Mollusca: Bivalvia: Lucinidae): Paleontology, v. 52, p. 95-109.

Teichert, B. M. A., Gussone, N., Eisenhauer, A., and Bohrmann, G., 2005, Clathrites: archives of a near-floor pore-fluid evolution ($\delta^{44/40}$Ca, δ^{13}C, δ^{18}O) in gas hydrate environment: Geology, v. 33, p. 212-216.

Torres, M. E., Wallmann, K., Trehu, A. M., Bohrmann, G., Borowski, W. S., and Tomaru, H., 2004, Gas hydrate growth, methane transport, and chloride enrichment at the southern summit of Hydrate Ridge, Cascadia margin off Oregon: Earth and Planetary Science Letters, v. 226, p. 225-241.

Ussler, W. and Paull, C. K., 2001. Ion Exclusion Associated With Marine Gas Hydrate Deposits, in: Paull, C.K., Dillon, W.P. (Eds.) Natural Gas Hydrates: Occurrence, Distribution, and Detection. AGU Geophysical Monograph 124, 41-51.

Ussler, W., and Paull, C. K., 2008, Rates of anaerobic oxidation of methane and authigenic carbonate mineralization in methane-rich deep-sea sediments inferred from models and geochemical profiles: Earth and Planetary Science Letters, v. 266, p. 271-287.

Wang, J., Jiang, G., Xiao, S., Li, Q., and Wei, Q., 2008, Carbon isotope evidence for widespread methane seeps in the ca. 635 Ma Doushantuo cap carbonate in south China: Geology, v. 36, p. 347-350.

FIGURE CAPTIONS

Fig. 1)

Structural sketch map of northwestern Italy (modified from Bigi et al., 1990) and location of the studied area.

Fig. 2)

Geological map (modified from Ghibaudo et al., 1985) (left) and stratigraphic section (right) of the upper Miocene sediments of the Ripa dello Zolfo area. Location of the map in Fig. 1

Fig. 3)

Block diagram showing the distribution of the carbonate-rich rocks discussed in the text. Symbols as in Fig. 2

Fig. 4)

Lucina-bearing mud breccias:

A) Outcrop view of the cemented rock body. The white dotted line shows the boundary with the hosting sediments.

B) Polished slab of the cemented mud breccias. Clasts of different size, floating in a darker fine-grained matrix, are recognizable. Small articulated and disarticulated bivalve shells (arrows) are also visible.

C) External mold of a *Lucina* bivalve.

D) Photomicrograph of a fracture cutting the matrix of the mud breccias. A fibrous aragonite rim, growing on micritic internal sediments, is recognizable.

Fig. 5)

Stratiform concretions:

A) Outcrop view of stratiform concretions. Three superposed dm-thick cemented beds with a lateral continuity of several meters (arrows) are recognizable under the snow. Location in Fig. 3.
B) SEM image of a broken chip of an homogeneous concretion body, showing the euhedral dolomite crystals cementing the sediments (slightly etched surface).
C) SEM image of pyrite framboids in an homogeneous concretion body (slightly etched polished surface).
D) Photomicrograph of a sand-sized quartz grain surrounded by a circumgranular rim filled with dolomite cement.

Fig. 6)
Septarian-like cracked concretions:
A) Outcrop view of the septarian-like cracked concretion described in the text. Note the sharp boundaries with hosting sediments and the wavy geometry.
B) Polished slab, cut perpendicular to bedding, of the septarian-like cracked concretion. Note the dense network of mm to cm- wide sediment-filled fractures developed both parallel and perpendicular to bedding. Most fractures taper out downward and do not reach the external surface of the concretion.
C) Polished slab, cut perpendicular to bedding, of the upper part of the concretion. Note the wedge-shaped empty fissures that taper out toward the upper surface and open toward the central part of the concretions (lower part of the image).
D) Photomicrograph of cross-cutting sediment-filled cracks. Different generations of sediment infilling are recognizable on the basis of color, content and size of terrigenous grains. Note alignment of elongated muddy clasts to the crack walls.

Fig. 7) Cement-filled cracks

A) Polished slab, cut perpendicular to bedding, showing some mm-wide cement-filled cracks (arrows). Note that the large crack in the central part of the image is only partially filled with cement.

B),C) Transmitted light (B) and cathodoluminescence (C) photomicrographs of cement infilling. In B) the first isopachous dolomite rim around the crack (arrows) and the zoning of later cements, evidenced by the alternation of more or less turbid layers, are recognizable. In C) cement banding is much more clearly recognizable. Note the lateral pinchout terminations (arrows) of dull to moderate orange cement zones against the bright yellow dolomite rim (D).

Fig. 8

A) Outcrop view of brecciated concretions. Note the partial overlap of the two layers and their lateral tapering off.

B) Polished slab, cut perpendicular to bedding, of the upper layer of Fig. 8A. Note that the edges of the clasts commonly fit together. The cement filling the interclast space is also visible.

C) Photomicrograph of the breccia. The dotted line indicates the outer boundary of a clast. It partly consists of microbreccia with elongated clasts that represent a sediment filled crack (compare with Fig. 6D). The sparry Mg-calcite cement (cc) filling the interclast space is also visible. The arrows indicate the early isopachous rim of dolomite developed along the periphery of two clasts.

D) SEM image of a broken chip cut at the boundary between a clast and the surrounding calcite cement (see Fig. 8C for location). The dolomite rim developed around the clast is recognizable (arrows). Due to the gently etch of the sample by HCl, dolomite is in relief with respect to calcite (cc).

F) Cylindrical concretion: note the regular cylindrical shape and the sharp boundaries with the hosting sediments.

G) Axial polished slab of a cylindrical concretion, showing the darker fill of the axial portion (dotted line). The white arrow indicates a clast wrenched from the walls.

Fig. 9)

Cross-plot of isotope data of Ripa dello Zolfo carbonate-rich rocks.

Fig. 10)

Sketches showing the filling mechanism of the fissure reported in Figs 7B and 7C. (I) An open fissure is occupied by gas hydrates (II). The progressive destabilisation of gas hydrates (III) leaves open voids that are filled with dull brown to orange zoned cements with diagnostic lateral pinchout terminations (IV, V and VI). For sake of simplicity, generation of voids after stage IV is omitted. White areas: open voids; GH: gas hydrate. For further details see text.

Fig. 11)

Evaluation of gas hydrate stability in the Tertiary Piedmont Basin (modified from Bohrmann and Torres, 2006)

A) Stability field of methane hydrates as defined by temperature and pressure (expressed as water depth) described in the text.

B) Thickness of the gas hydrate stability zone at 500 and 1000 m water depth. For further details, see text.

Fig. 12)

Sketches illustrating the two phases of methane flow discussed in the text. GH: gas hydrates. Arrows indicate the flow path of CH_4-rich fluids.

A) First episode, responsible for the formation of *Lucina*-bearing mud breccias (MB) and of the cylindrical concretions hosted in the lower part of the studied section;

B) Second episode, giving rise to stratiform concretions (SC) and to cylindrical concretions hosted in the upper part of the studied section.

Fig. 13)

Schematic evolutionary model of concretion formation. For further details see the text.

A) Left: upward flow of CH_4-rich fluids (arrows) and formation of an homogeneous concretion (HC); right: contraction of sediments, resulting in a network of secondary fissures.

B) enlargement of fissures by forceful mud injections (stippled grey) and gas hydrate (GH) crystallization; GHSZ: gas hydrate stability zone.

C) Upward shift of the base of the GHSZ, and precipitation of dolomite both in the sediment-filled fissures and on the walls of the empty ones (DR = dolomite rim).

D): Downward shift of the base of GHSZ and new phase of formation of gas hydrates.

E) Progressive destabilisation of gas hydrates and precipitation of zoned calcite cements (ZCC) in the septarian-like cracked concretion (SC). For sake of simplicity, empty fissures within SC are not represented.

F) destabilisation of gas hydrates at shallow burial depth and production of brecciated concretion (BC); CC: cylindrical concretions

Table 1: Stable isotope data of the Ripa dello Zolfo carbonate-rich rocks .

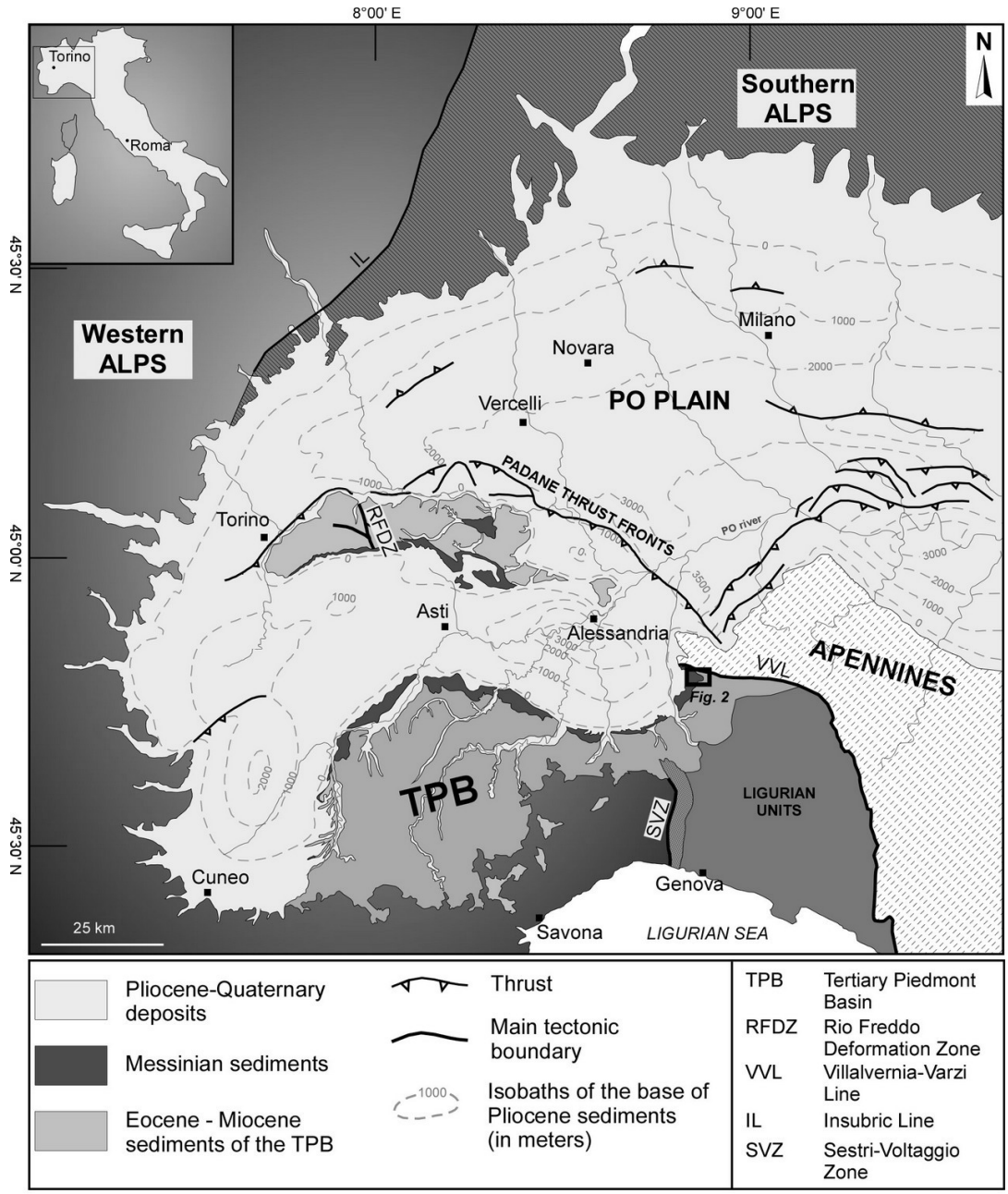

Dela Pierre et al.
Fig.1.JPG

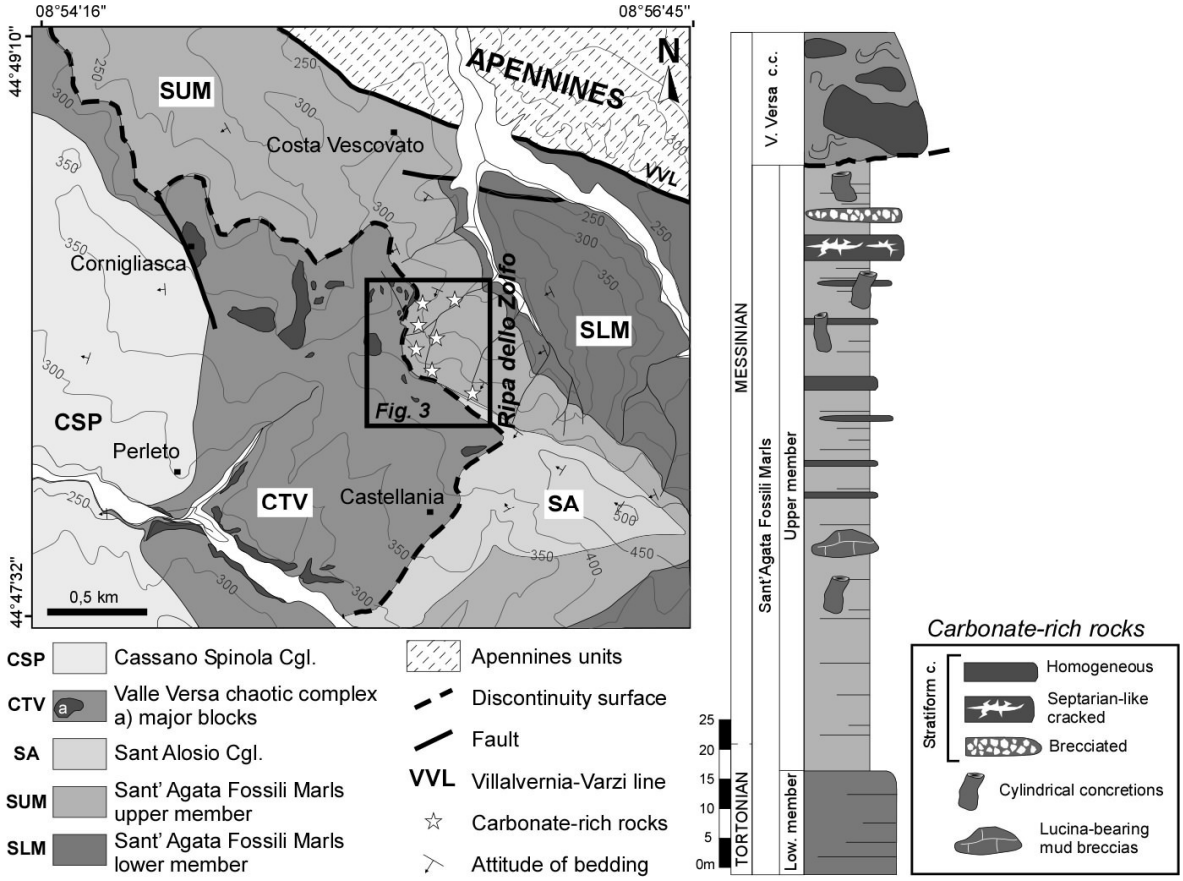

Dela Pierre et al.
Fig.2 .JPG

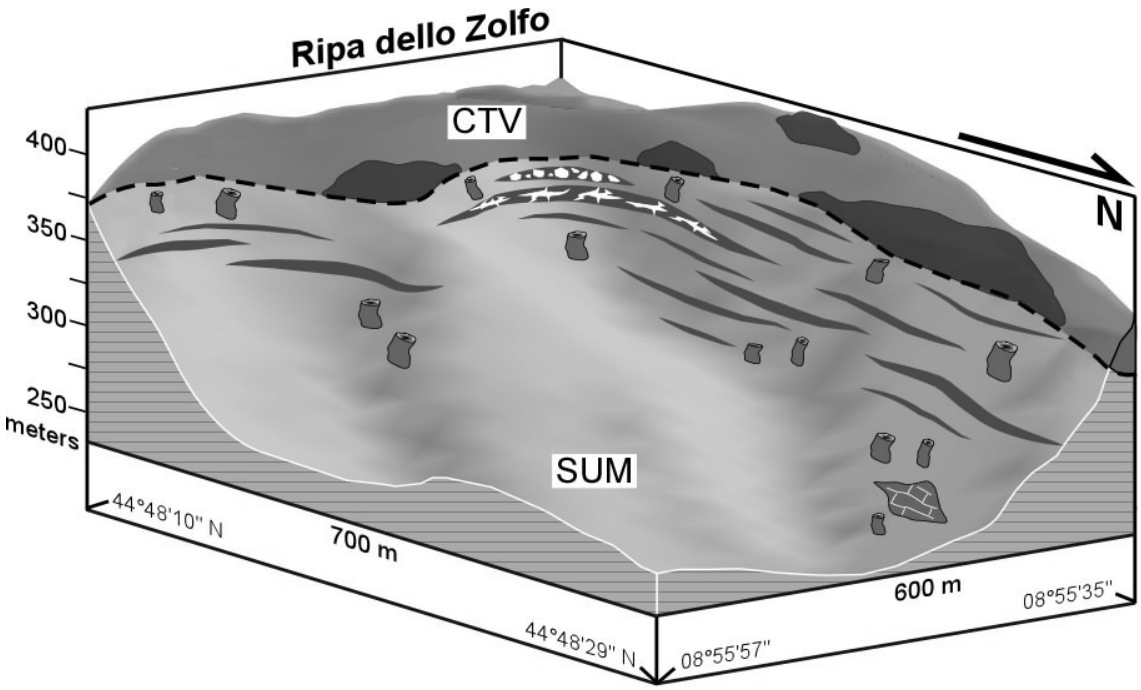

Dela Pierre et al.
Fig.3. JPG

1

2

3

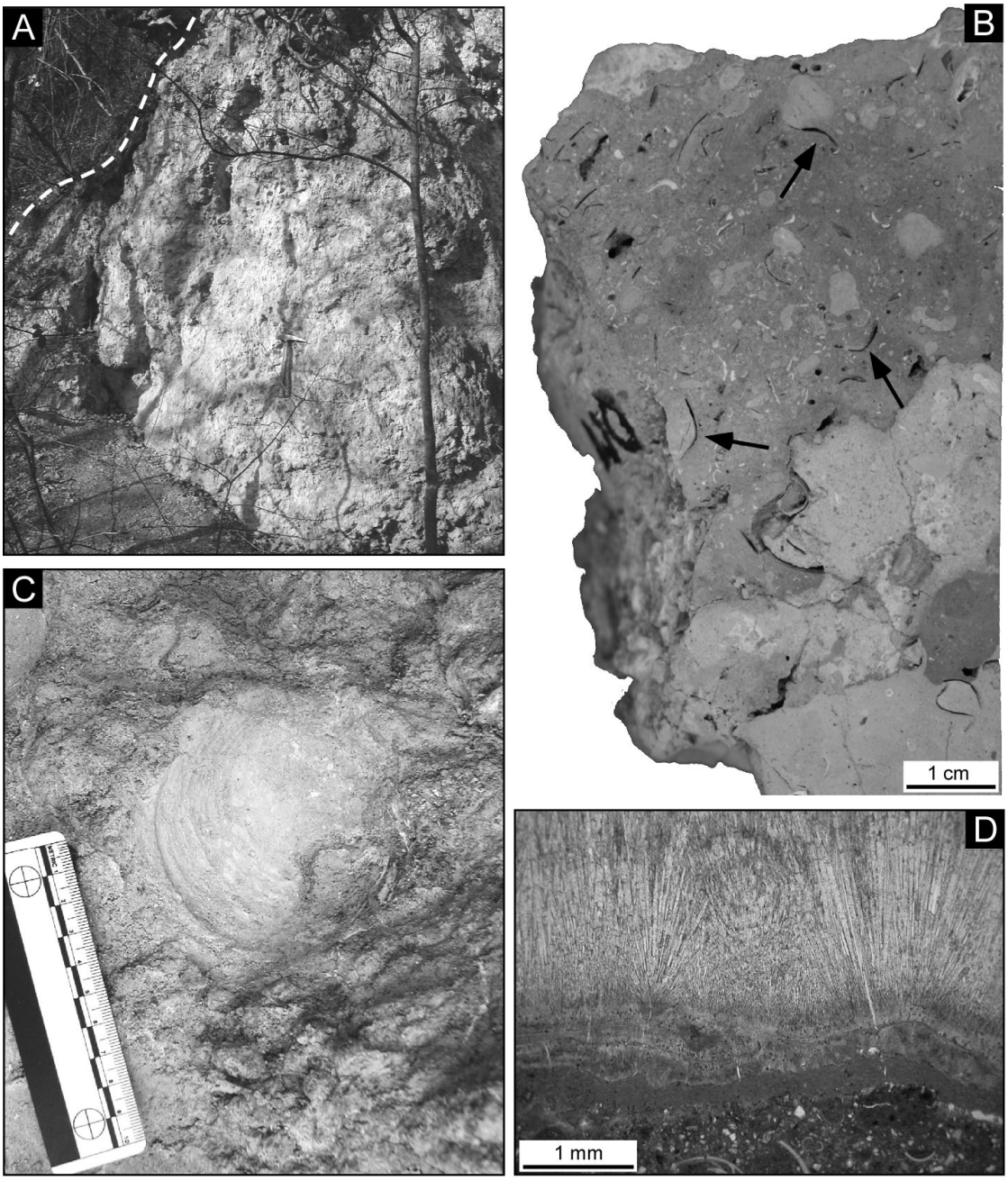

Dela Pierre et al.
Fig.4 .JPG

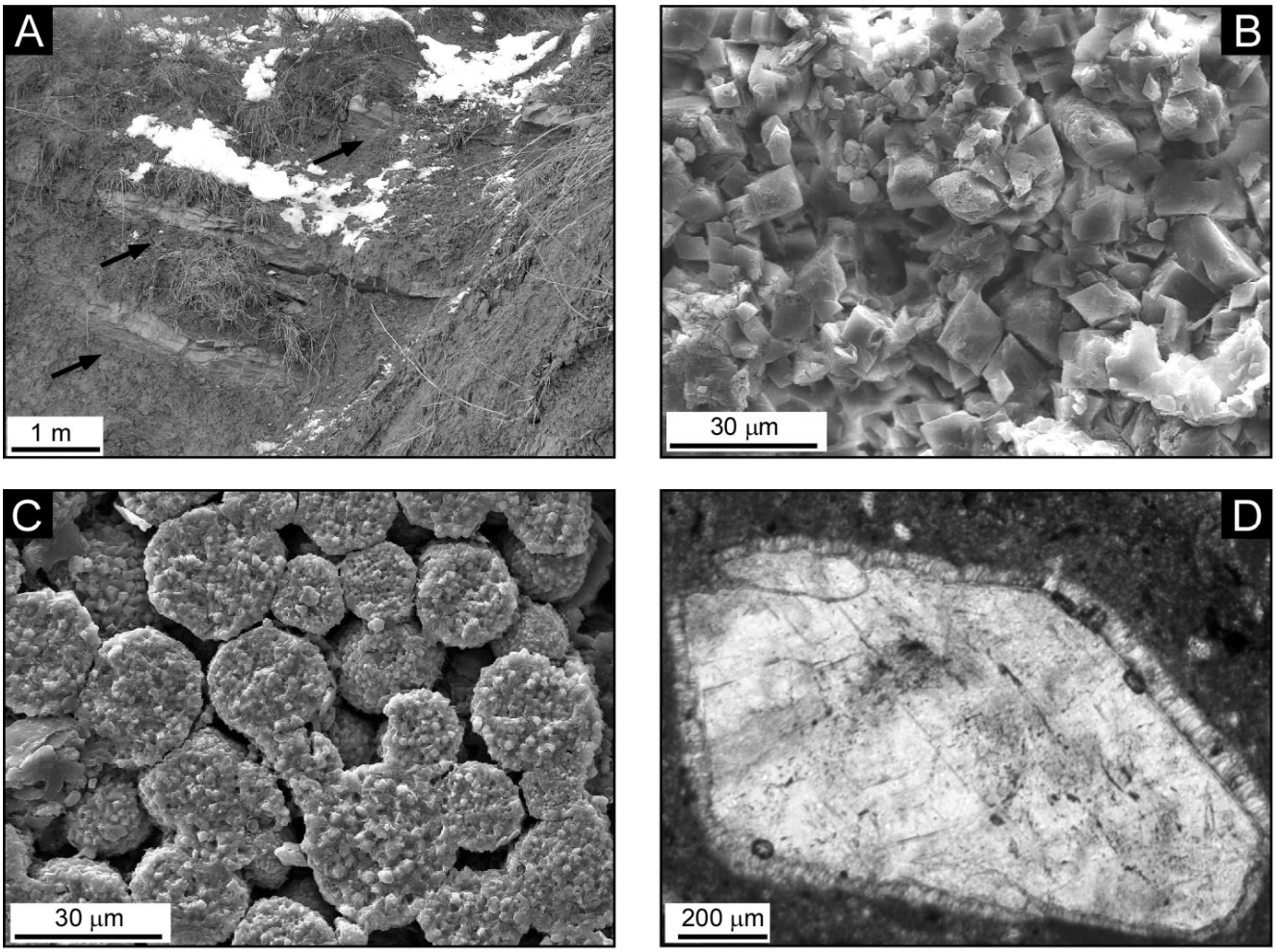

Dela Pierre et al.
Fig.5 .JPG

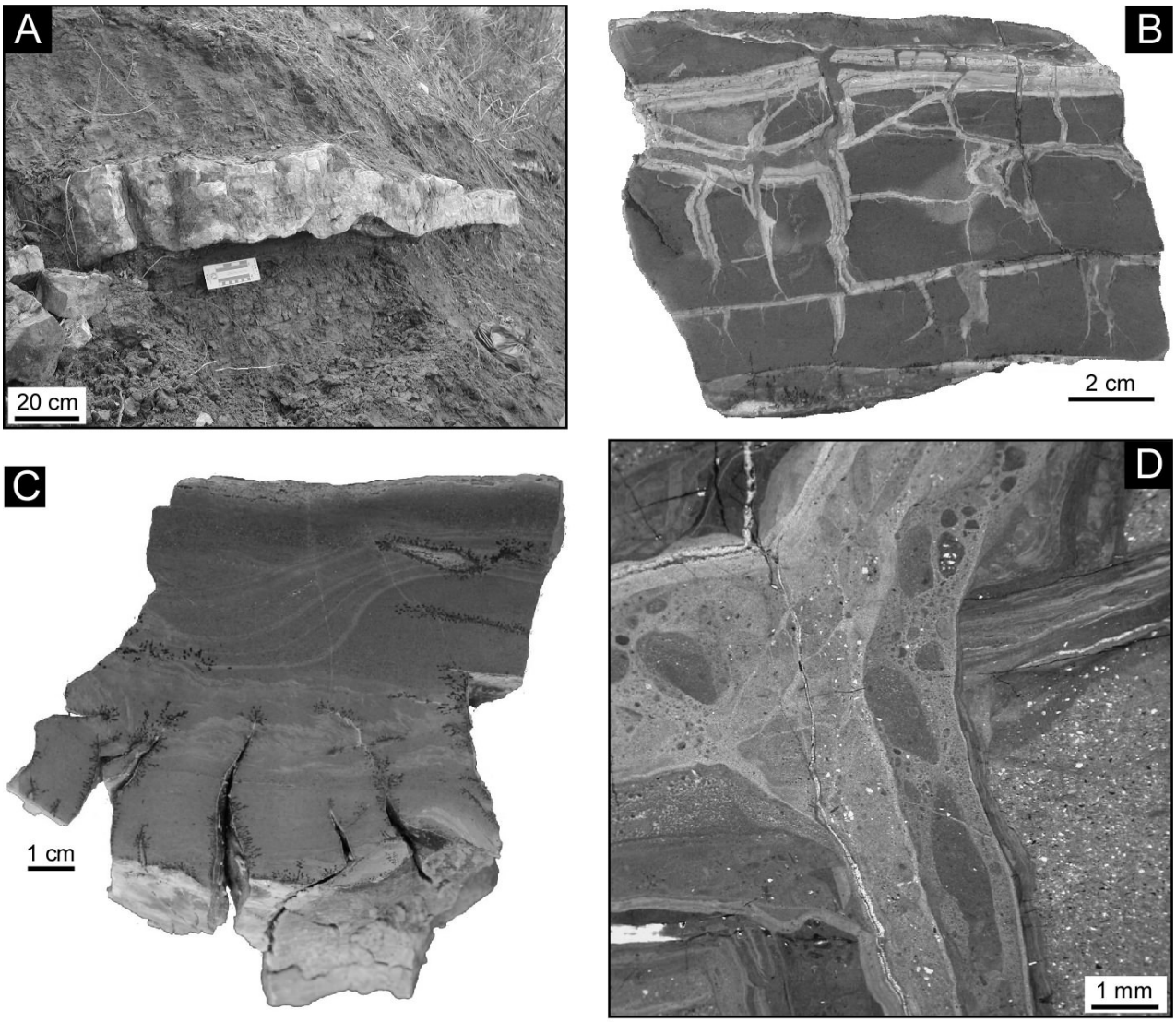

Dela Pierre et al.
Fig.6 .JPG

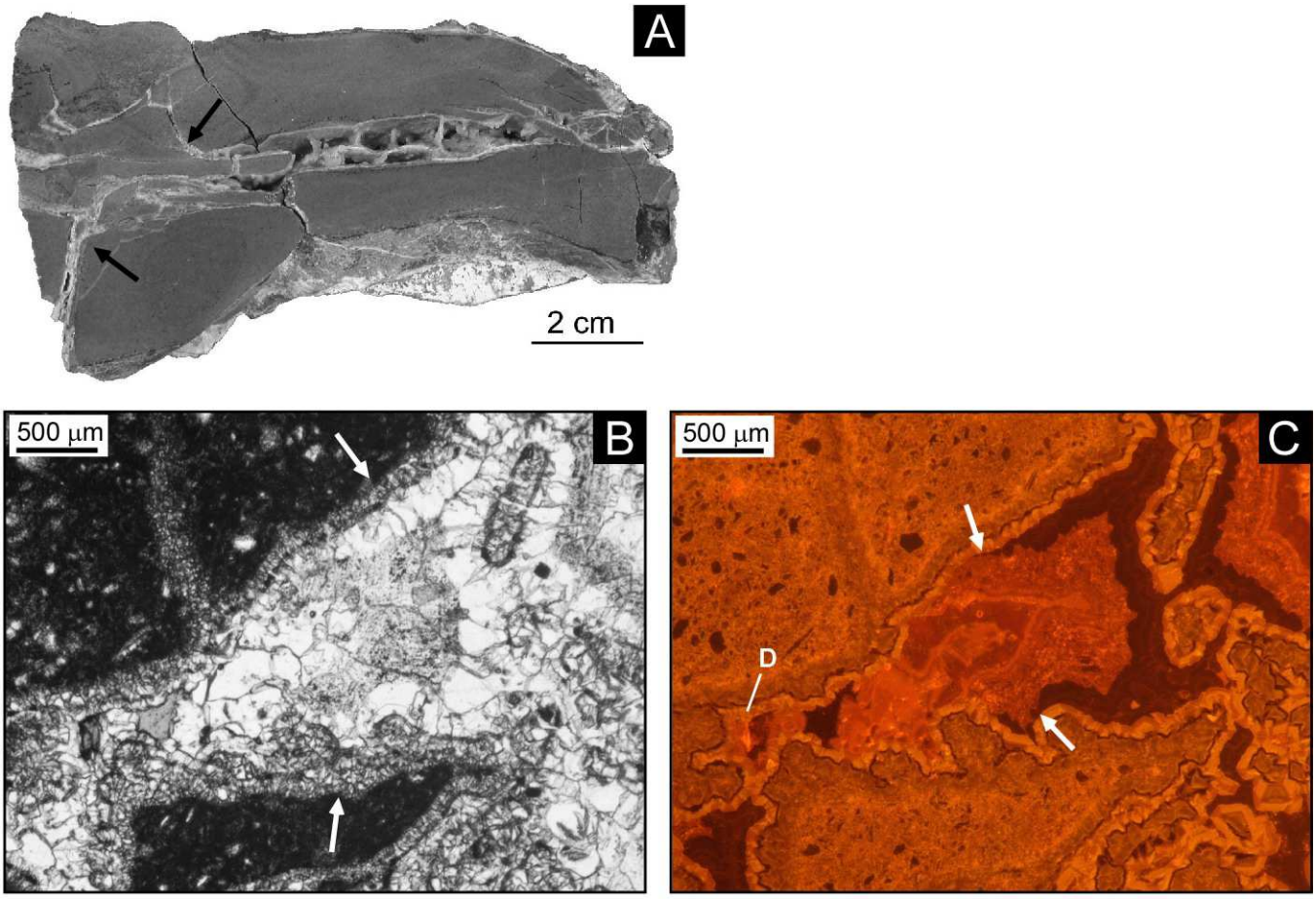

Dela Pierre et al.
Fig.7 .JPG

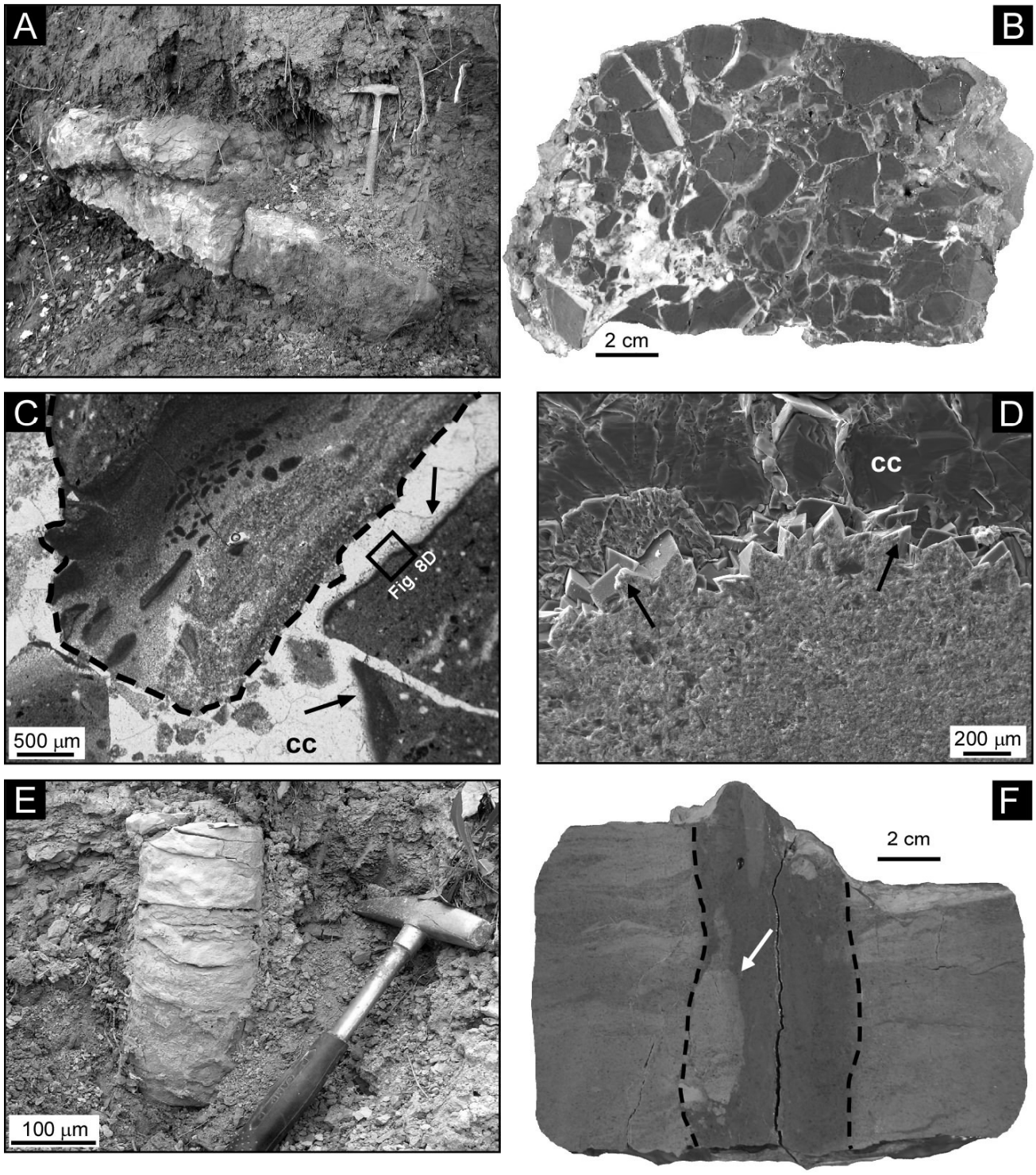

Dela Pierre et al.
Fig.8 .JPG

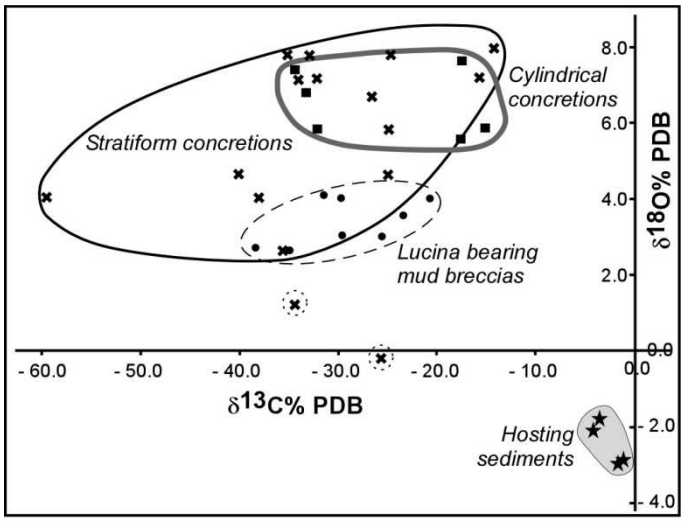

Dela Pierre et al.
Fig.9 .JPG

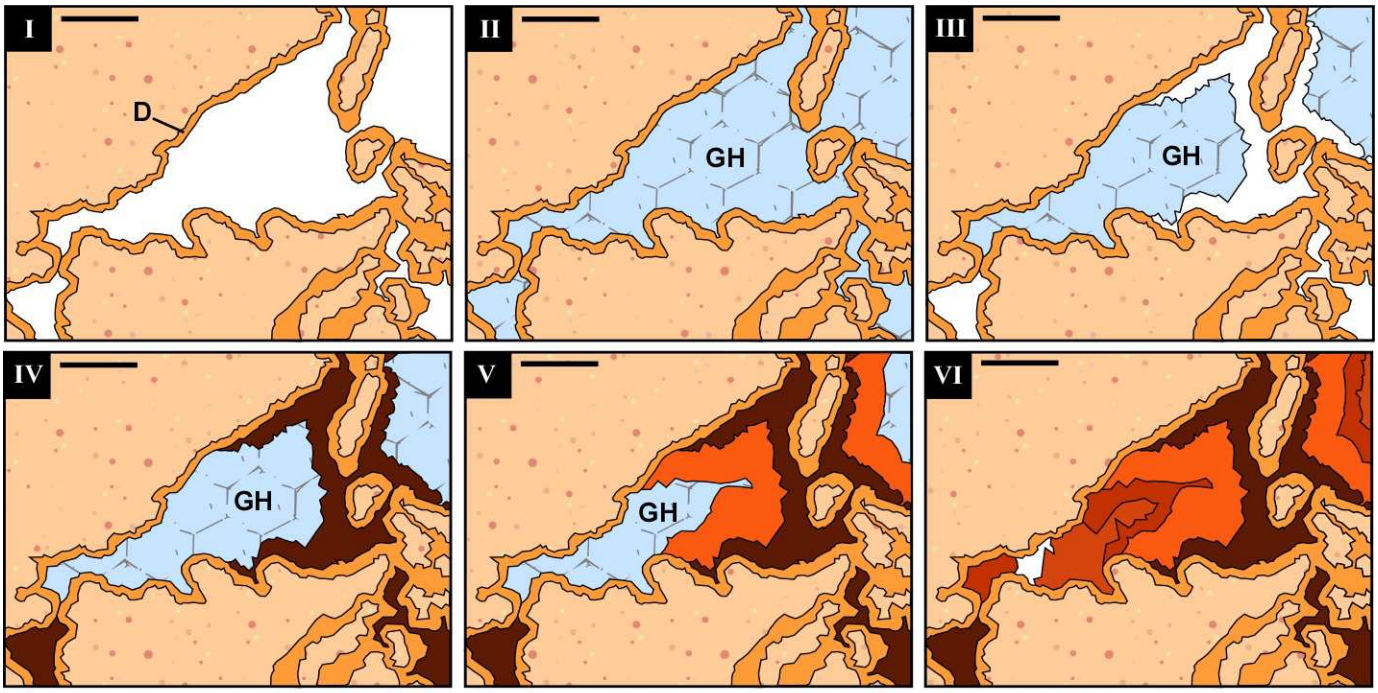

Dela Pierre et al.
Fig.10 .JPG

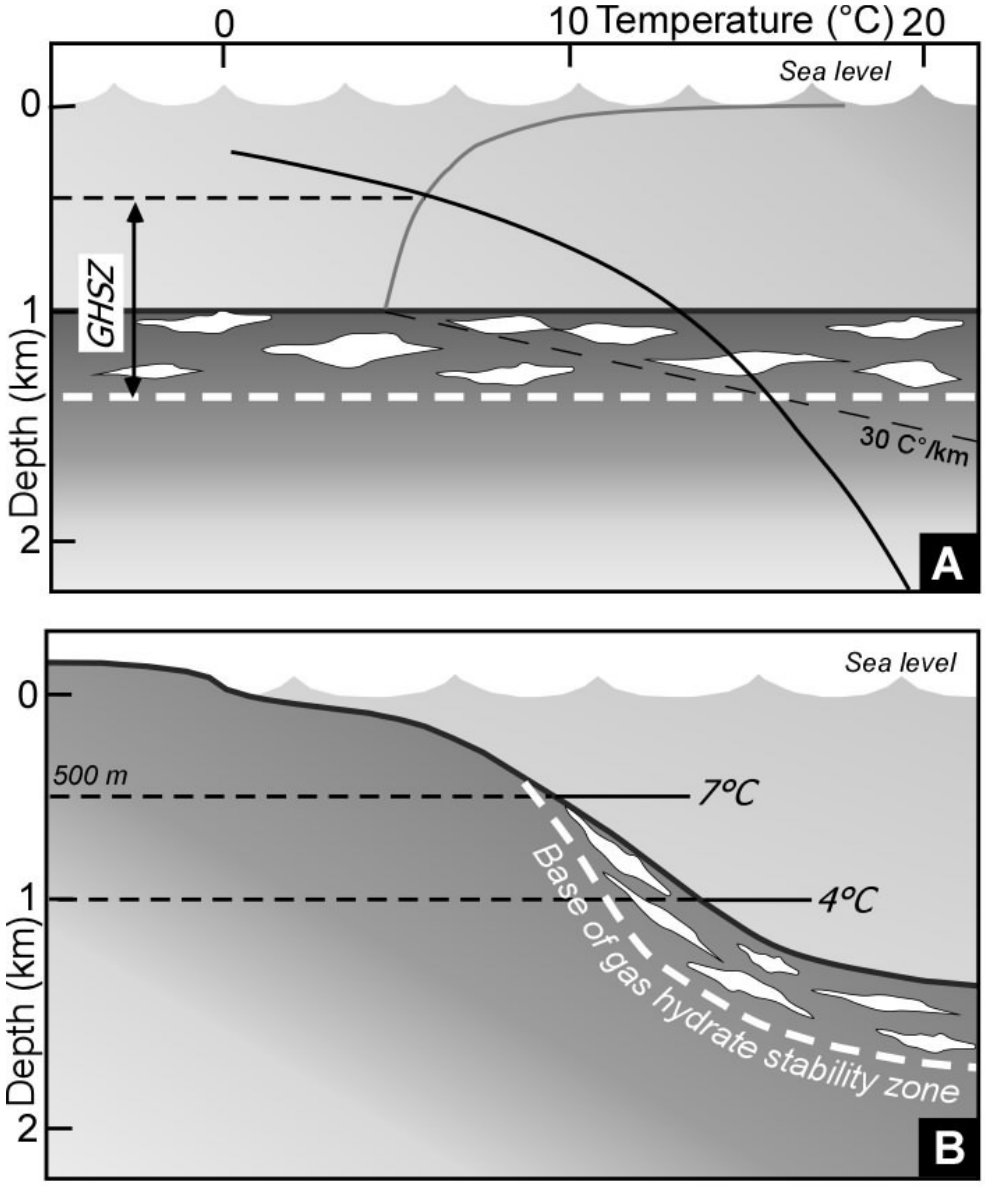

Dela Pierre et al.
Fig.11 .JPG

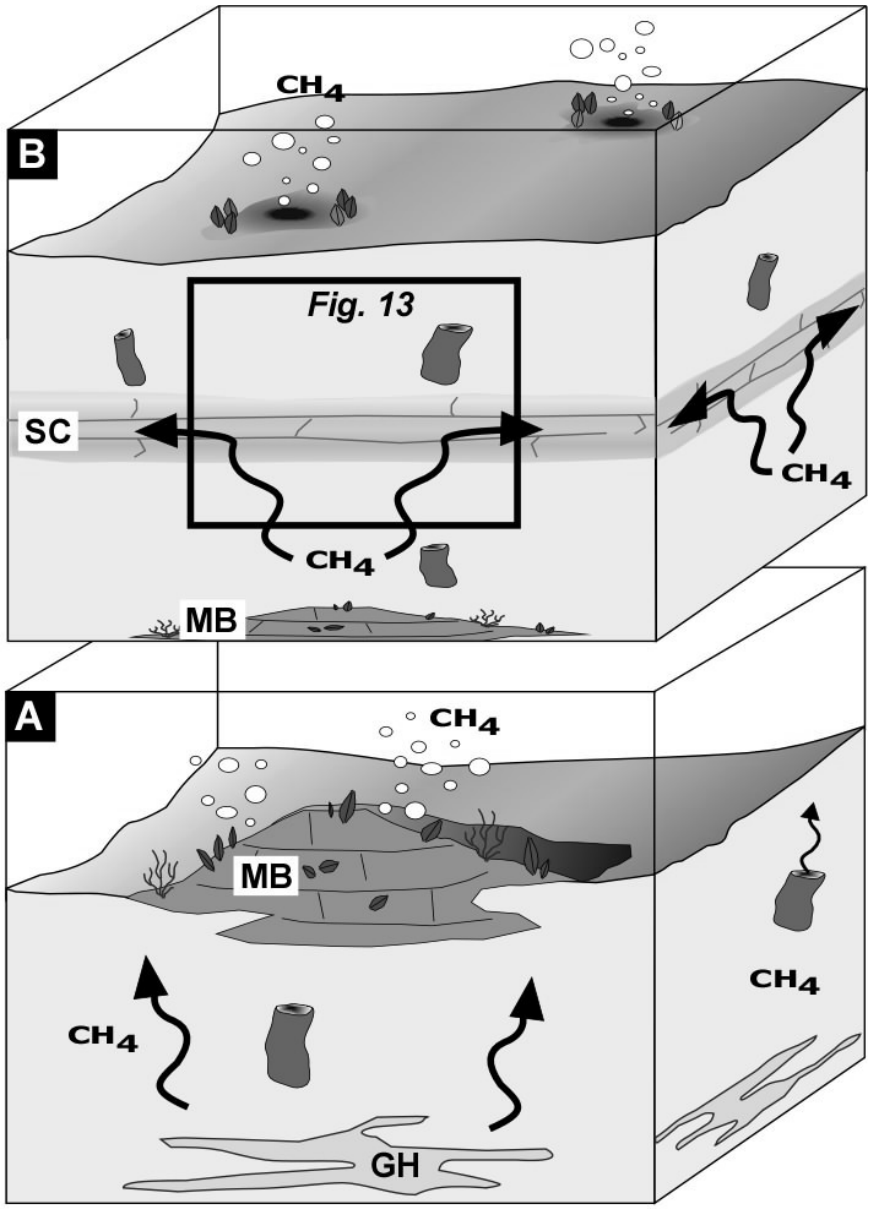

Dela Pierre et al.
Fig.12 .JPG

1
2

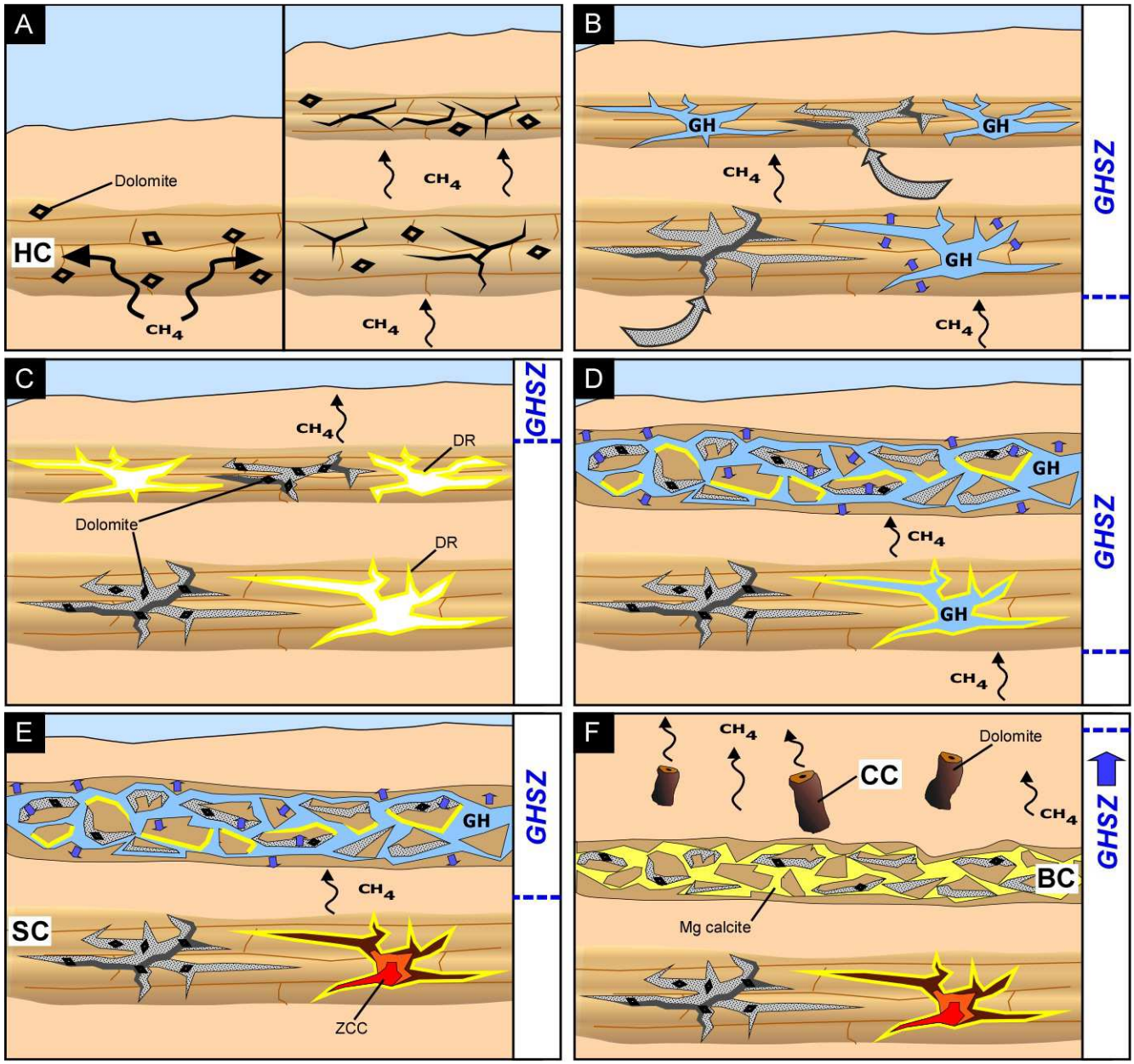

Dela Pierre et al.
Fig.13 .JPG

3
4

TABLE 1. THE CARBONATE-RICH ROCKS STABLE ISOTOPE DATA

Sample number	∂13C (‰ PDB)	∂18° (‰ PDB)	Sample type	Carbonate mineralogy
Hosting sediments				
DM103	-3.5	-1.8	Silty marls	Calcite
DM133	-4.1	-2.1	Silty marls	Calcite
DM134	-1.7	-3.0	Silty marls	Calcite
DM135	-1.1	-2.8	Silty marls	Calcite
Lucina bearing mud breccias				
ZF121B	-25.6	3.0	Clast	Calcite
ZF122B	-20.7	4.0	Clast	Calcite
ZF120A	-29.6	3.1	Matrix	Calcite
ZF121A	-23.4	3.6	Matrix	Calcite
ZF122A	-31.5	4.1	Matrix	Calcite
ZF123B	-29.8	4.0	Matrix	Calcite
ZF115B	-38.4	2.7	Fracture-filling cement	Aragonite
ZF120B	-35.0	2.6	Fracture-filling cement	Aragonite
Stratiform concretions: homogeneus				
Z12	-59.6	4.0	Concretion body	Dolomite
ZF1	-40.1	4.7	Concretion body	Dolomite
ZF3	-35.6	2.7	Concretion body	Dolomite
ZF9	-38.0	4.0	Concretion body	Dolomite
ZF15	-34.0	7.1	Concretion body	Dolomite
Stratiform concretions: septarian-like cracked				
ZF103A	-26.6	6.7	Concretion body	Dolomite
DM44	-32.9	7.8	Concretion body	Dolomite
DM78	-24.7	7.8	Concretion body	Dolomite
DM115-1	-35.1	7.8	Concretion body	Dolomite
ZF103B	-34.4	1.2	Fracture-filling cement	Calcite
ZF106B	-32.2	7.2	Sediment-filled crack	Dolomite
Stratiform concretions: brecciated				
Z11a	-25.7	-0.2	Clast	Dolomite
Z11b	-15.7	7.2	Clast	Dolomite
DM118-1	-13.8	7.9	Clast	Dolomite
ZF109B	-25.0	4.7	Inter-clast cement	Mg-calcite
DM118-2	-24.7	5.9	Inter-clast cement	Mg-calcite
Cylindical concretions				
RDZT1a	-32.1	5.9	Axial portion	Dolomite
RDZT2a	-15.1	5.9	Axial portion	Dolomite
RDZT1b	-33.2	6.8	Concretion body	Dolomite
DM17	-17.6	5.6	Concretion body	Dolomite
RDZT2b	-17.5	7.6	Concretion body	Dolomite
ZF5	-34.3	7.4	Concretion body	Dolomite

Dela Pierre et al.
Table 1 .DOC